Universidad de las Américas Puebla

Actuarial Sciences, Physics and Mathematics Department

Quantum Chaology Manifestations in Simple Rare-Earth Metal Electronic Structures

Thesis presented by the student

Eric Macedo Esparza

with student ID 151075

as required by the Honors Program of the

Universidad de las Américas Puebla

Supervised by

Dr. Miguel Angel Ocaña Bribiesca

2018

Abstract

We present the statistical analysis of the energy band structures of the Si and Eu crystals. This analysis was done to determine whether Eu manifests quantum chaology or not in its energy spectrum in the same way that Si does. This analysis gives further insight into the possible effects that the f orbitals have on the band spacing distribution such as the strong on-site Coulomb interactions. Furthermore, Hubbards U parameter proved to be an important factor in the correction of the model in order to obtain a more accurate calculation of the Hohenberg-Kohn functional. We find that our results for Si are in good agreement with those of Mucciolo et al. The results for Eu do not agree with those of Mucciolo et al. and are analyzed more thoroughly with velocity distributions.

Acknowledgements

Firstly, I would like to thank my thesis advisor Dr. Miguel Angel Ocaa Bribiesca. The door to his office was always open whenever I ran into a problem or had a question about my research or writing. He was always there for me and I cannot thank him enough.

I would like to thank my friends for always being there through the tough times. I could always count on their help and support whenever I was having a hard time and I appreciate everything they have done to help me out.

A special thanks to my parents who have always supported my education and all my aspirations of becoming a scientist even when big obstacles were on the way they were there to help me push forward. I couldn't have become who I am without you.

Finally, I'd like to thank my brother who taught me to question everything and ultimately have my own opinion about things. I believe I owe my scientific mind to him!

Chaos: When the present determines the future, but the approximate present does not approximately determine the future

Edward Lorenz

Contents

List of Figures

Chapter 1

Introduction

Ever since Newton and Laplace, physics had been thought of as a deterministic field since one could clearly *determine* the future and past trajectories of macroscopic objects or, more importantly, celestial bodies. By observing a celestial body at a given time one could quite accurately approximate its future and past positions, knowledge that was used freely in many civilizations in order to instill fear, prove divinity or even improve agricultural processes (such as ancient civilizations (Welser-Sherrill, 2007)). It wasn't until physicist Ludwig Boltzmann studied gases and began to formulate *statistical physics*(Oestreicher, 2007) that a non-deterministic point of view was beginning to take form. The phenomenon known as "chaos" was first noted in 1961 by physicist Edward Lorenz from the Massachusetts Institute of Technology (MIT) and officially discovered two years later by himself while doing research about the weather(Oestreicher, 2007).

Unlike classical mechanics, quantum mechanics has eluded deterministic ideals since the very beginning due to Heisenberg's uncertainty principle, and it is because of this very concept that chaos cannot be treated in quantum mechanics in the same way. According to Michael Berry(Berry, 1989), 'quantum chaos' is a term which can mostly be misinterpreted and thus uses the phrase 'quantum chaology'. For the purposes of quantum theories, one must then use another mathematical tool called a random matrix in order to study chaos in the quantum realm.

Random Matrix Theory began in 1951 when physicists Eugene Paul Wigner and Freeman Dyson began to make statistical analyses in nuclear physics, something that had not been done before. Wigner laid the foundations of RMT within nuclear physics and opened a door to many other applications within physics such as the fractional quantum Hall effect(Callaway, 1990), quantum chromodynamics(Akemann,

2016), or superconductors.

One of the many advantages of using this theory over others was due to the lack of chaotic fluctuations, those present in classical mechanics, one had to deal with averages due to a phenomenon known as *supression of chaos*(Berry, 1989). This meant that phycisists or mathematicians alike could not mathematically deal with chaos as had been done in classical systems. One of the things Berry mentions is that this suppression happens due to wavefunction morphologies, something specific to quantum mechanics, and thus we must look at quantum chaos (quantum chaology) in a semi-classic point of view. Random Matrix Theory is especially important because three different ensembles, known as the Gaussian ensembles, are the ones used within literature to compare and determine whether a system manifests chaos or not.

This thesis focuses on proving whether the electronic structure of Eu manifests chaos or not and compares it to the electronic structure of Si that does manifest chaos(Mucciolo et al., 1994). Because the focus of the thesis is not to obtain analytic results about chaos or its role within the systems, there is no further analysis into the formalisms and specificities of the subject. GOE ensembles are used as a major tool and theory to support the numeric results obtained through simulations of energy level spacing of these elements. In order to obtain these numeric results, Density Functional Theory (DFT) is applied through a computer program called WIEN2k(Blaha et al.). Similarly, DFT is studied superficially in order to understand what calculations are done by the WIEN2k program and what they mean and so the theory is not studied in great detail and no further analysis is done.

Chapter 2 presents an introduction to chaos, random matrix theory (RMT), and density functional theory (DFT). We first introduce chaos, its defining points and the connection it has with random matrices. Afterwards, density functional theory is introduced along with the quantum physics it is based on.

Chapter 3 is focused on the analysis of the results obtained from the DFT calculations done by the Wien2k program and the FORTRAN code created for the band spacing distributions for Si and Eu.

Finally, the conclusions present the accomplishments of the work as well as any further comments. Important results of the work, including possible further research is explored.

Chapter 2

Theoretical Background

The electronic structure of an atom or molecule is one of, if not the most, important aspect to analyze. The reason for this is that depending on the amount of electrons available in a Valence shell, atoms or molecules will interact in a very specific ways between themselves. While Newtonian mechanics may describe celestial (referring to astronomical objects like stars, comets, asteroids, planets, etc.) and everyday dynamics with outstanding precision, they are not able to describe very small systems well ("small" is a relative term and so we'll say sizes around 100nm or smaller) just like the electronic structures of atoms. This is because atoms and particles do not behave in the same way as our everyday objects do. Because of this, one must use the laws of Quantum Mechanics to accurately describe and understand the systems being dealt with. Within this thesis we will specifically deal with electronic structures and thus must abide by the quantum theory. Before getting into the quantum theory we must first look at the basics of *chaos* and how it got tied into quantum systems.

2.1 Dynamical Systems and Quantum Chaos

For the past century many scientists have been very keen on deciphering chaos; the random, the unpredictable, the ever changing. So far, chaos has evaded analytical descriptions for the most part and has mostly been described through qualitative means(Boeing, 2016).

To study and ultimately understand chaos one must first look at dynamical systems and under what conditions they are chaotic. A *dynamical system* is defined as as "a system whose state evolves with time over a state space according to a fixed rule"(Nykamp). In addition to this, dynamical systems depend solely on their

current state when evolving in time. Since dynamics studies the progression of a system in time, this area has been studied for centuries, specifically since Newton created calculus and was able to describe such systems. Later on it was discovered that these systems could be classified into *linear* and *nonlinear* systems.

Linear systems satisfy the superposition principle and can generally be predicted by knowing the initial conditions(Boeing, 2016). The fact that these systems satify the superposition principle is important because a seemingly complex behavior can ultimately be separated into its simpler components and still be described entirely. By contrast, a nonlinear system is that in which, according to Geoff Boeing, "[...]the whole becomes something greater than the mere sum of its individual parts"(Boeing, 2016). While this idea may be rather counter-intuitive, it does shed a light on some basic intrinsic ideas about chaos such as its unpredictability and self-similarity in some cases (such as fractals) in which there is no repetition whatsoever. This ultimately means that any interactions with this kind of system will act nonlinearly and in a rather complex manner. Because nonlinear systems cannot be broken down into simpler problems just like linear systems, they become quite difficult to solve analytically.

In order to more explicitly show the difference between a linear and non linear dynamical system some basic examples are shown. A linear dynamical system could be something of the sort:

$$\dot{x}_3 = \alpha x_1 + \beta x_2 \tag{2.1}$$

It is quite clear that the system is linear because all the x's are linear terms and have no quadratics or other type of behavior. Comparatively, a nonlinear system would be

$$\dot{x}_3 = \gamma \sin x_1 + \epsilon \exp x_2 \tag{2.2}$$

since the $\sin x$ function and the exponent aren't linear functions of x.

Ever since the 1950s with the rise of computers, most advances in research within the field have been of a numeric and visual nature(Strogatz, 1994). An example of this is Figure 2.1 which shows a bifurcation logistic map that doesn't start out chaotically yet after a few iterations of the model, one can notice that there is somewhat of an "explosion" or boom of activity in the system and almost instantly becomes rather unpredictable. Within nonlinear dynamical systems exist *chaotic* systems. These systems are extremely sensitive to initial conditions and due to this

any interactions, no matter how small, will affect the system greatly. As mentioned before, since the system depends solely on its current state, chaotic systems in a specified state cannot provide any useful information about very close-valued or similar states since the initial condition is different. In other words, in a state space while analizing a specific point you cannot say anything about any adjacent points even if everything about the initial point is known. At this point it is important to note that chaotic nonlinear systems are still deterministic systems in the sense that the randomness is not due to noise or random external input but rather it is due to the actual nonlinearity of the system. This is one of the main reasons that quantum chaos cannot be describd in the same way as classical chaos, since quantum mechanics is intrinsically non-deterministic due the uncertainty principle and the underlying probabilistic approach.

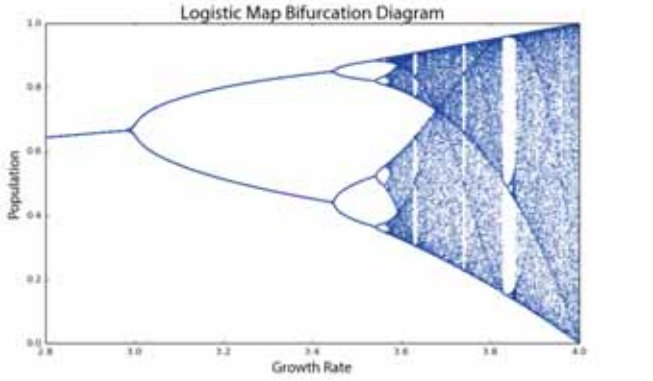

Figure 2.1: Bifurcation logistic map: one of the most famous visual analyses of a chaotic system.

Classically, to determine chaoticity of a system (whether they are chaotic or not or even *how* chaotic they are) one must use the Lyapunov(sometimes also spelled Liapunov(Strogatz, 1994)) exponent. This is to determine *how* sensitive the dynamical system really is. This is done by comparing near trajectories (dynamics in which the system's initial condition is slightly changed) and analyzing how much they differ from each other and it is one of the most direct ways to "test" the chaoticity of the system. Since this method requires strange attractors, deterministic systems and differential equations we will not delve deeper into the topic as we must instead look into the tools necessary for quantum systems.

Quantum systems have been compared to their classical counterparts in order to further understand the quantum realm because studying already known systems is much easier. One of the many things that were being compared was the way in

which chaos manifested itself in the quantum realm. Chaos does not exist quantum-mechanically in the same way as it does classically due to something called *suppression of chaos*(Berry, 1989). This phenomenon is studied when looking at what is known as the semiclassical limit of quantum mechanics. The semiclassical limit according to Micheal Berry is when Planck's constant, h, equals zero and quantum mechanics is,"[...] essentially singular at the classical origin."(Berry, 1989). He argues that the classical limit of quantum mechanics, "[...] conceals a rich variety of phenomena". Since we are studying a quantum system we must be able to describe such a system's chaos correctly, yet we cannot approach the problem as is done in classical mechanics. Classically, there are two main approaches to nonlinear dynamics: differential equations and iterated maps (Strogatz, 1994). As mentioned by Strogatz, these two methods differ in how time behaves: differential equations deal with continuous time while iterated maps deal with discrete time. Within science and engineering the most used method is that of differential equations since we assume time is always continuous whereas in computational cases time is inherently discrete within the computers, thus a computer programmer might use the iterated map for computational processes of some sort.

So, as Strogatz(Strogatz, 1994) cleanly puts it, "chaos is aperiodic long-term behavior in a deterministic system that exhibits sensitive dependence on initial conditions". Yet, according to Michael Berry it does not exist in the same manner quantum mechanically(Berry, 1989) because they are inherently **not** deterministic due to Heisenberg's Uncertainty principle. Due to this, we must then use a different mathematical theory for quantum chaos (chaology). The leading mathematical entity being used to describe this phenomenon is known as **Random Matrix Theory**.

2.1.1 Random Matrix Theory

Random Matrix Theory was first introduced into nuclear physics by Eugene Wigner while studying nuclear spectra of heavy atomic nuclei. But, why study the statistical behavior of nuclei? According to Mehta (Mehta, 2004), "The statistical behaviour of the various energy levels is of prime importance" because one can characterize certain aspects of the nuclei such as fast and slow neutron reactions. Eventually this application of random matrices carried over to other branches of physics and has been used in many things such as the chaoticity, elastodynamic properties, and conductivity in disordered materials.

In slow nuclear reactions there are many nucleons involved whereas in the fast

reaction few are involved. The slow reactions are of interest because of the amount of constituents involved which means that varying energy levels will hence be taken into account. Ultimately, this means that the average properties of these energy levels need to be studied, such as the level spacings, radiation width and fission widths. We will only be working with level spacings in this work since we are not working with nuclei but rather with the electronic structure. Wigner postulated that the spacings between the lines in the spectra of the nuclei had to resemble the spacings between the eigenvalues of a random matrix(Mehta, 2004).

Wigner's postulate is a direct result from the base theory of quantum mechanics: the Schrödinger equation. In the Scrhödinger equation, the operator H is the Hamiltonian, the eigenfuntion ψ is the state of the system, and its eigenvalues ϵ are the energy.

$$H\Psi_i = \epsilon_i \Psi_i \tag{2.3}$$

Generally, quantum mechanics treats this in an infinite-dimentional space known as the Hilbert space, but we want to avoid having to calculate infinite dimensions in a real example, therefore in order to obtain good approximations statistical hypotheses on H using general symmetry properties since we will use a complete set of basis to represent the Hamiltonians as matrices. These Hamiltonians will then be the random matrices being used when working with the electronic structures. Dyson (Dyson and Mehta, 1963) stated that, "The statistical theory will not predict the detailed level sequence of any one nucleus, but it will describe the general appearance and degree of irregularity of the level structure that is expected to occur in any nucleus which is too complicated to be understood in detail". That means that any heavy nuclei such as the rare-Earth metals are excellent nuclei in which we can apply these methamatical tools.

As the name suggests, a random matrix is a type of matrix whose entries are random variables(Tao, 2012). Wigner proposed a simple system where the levels have the same spin, and parity as well as additional parameters given by the system. The random variables would then have to follow some distribution and Wigner assigned the Gaussian distribution. After some experimental data was obtained, Porter and Rosenzweig (Mehta, 2004) compared the Wigner assumptions and the Monte Carlo simulations only to prove his hypothesis right. Dyson then proved (Dyson and Mehta, 1963) that an ensemble of matrices that are invariant under a symmetry group must fall into three different categories: orthogonal, unitary and symplectic. These

three ensembles are currently known as the Gaussian Orthogonal Ensemble (GOE), Gaussian Unitary Ensemble (GUE), and the Gaussian Symplectic Ensemble. For the analysis of the electronic band structure energy spacings we will be using the GOE and the GUE exclusively.

Gaussian Ensembles

An important fact about the random matrices used is that they must be Hermitian, meaning that the adjoint of the matrix is the matrix itself:

$$H^{\dagger} = H \tag{2.4}$$

which means that the eigenvalues will be real. Moreover, as a result from the Monte Carlo simulations it was found that the diagonal elements of these matrices must have the same distribution(Mehta, 2004).

We must then look at each of the two ensembles we'll be dealing with independently, the GOE and the GUE. Each of these ensembles is used to treat systems with different symmetries so we must define the differences between them.

Overall, the main problem in random matrix theory is obtaining the probability distribution for the ensembles. Since we are working with known ensembles we will already know them. Additionally, RMT for Hamiltonians is based on very little information of the system itself apart from the symmetries it has. These symmetries ultimately impose certain restrictions on the Hamiltonian. Because of these restrictions we must then compare the two different ensembles in order to determine which one of the ensembles better resembles the results obtained from the DFT calculations.

Gaussian Orthogonal Ensemble

The Gaussian Orthogonal Ensemble (GOE) is one of the most studied ensembles and was first proposed by Wigner when studying the spectra of heavy nuclei. The GOE is defined by Mehta (Mehta, 2004) in the following way:

Definition 2.1 The Gausssian orthogonal ensemble is defined in the space of real symmetric matrices with the following two requierments:

- The ensemble is invariant under an orthogonal transformation by some orthogonal matrix M:

$$H' = M^T H M \tag{2.5}$$

- The elements H_{ij}, where $i \leq j$, in the matrix are all statistically independent. This means that the probability density is a product of functions that depend on one of the random variables of the matrix H:

$$P(H) = \prod_{i \leq j} f_{ij}(H_{ij}) \tag{2.6}$$

The distribution, as mentioned in the definition, is invariant under orthogonal conjugation and usually models Hamiltonians with time-reversal and rotational symmetry.

The distribution function of the GOE is the following(Haake)(Mehta, 2004)(Reichl, 1992):

$$P(s) = (\frac{s\pi}{2})e^{\frac{-s^2\pi}{4}} \tag{2.7}$$

Gaussian Unitary Ensemble

Unlike the GOE, the Gaussian Unitary Ensemble (GUE) is **not** time-invariant and thus can be any Hermitian matrix; it does not have to be real or self-adjoint as was the case with the GOE. The definition that arises is then the following (Mehta, 2004):

Definition 2.2 The Gaussian unitary ensemble is defined in the space of Hermitian matrices by the following:

- The ensemble is invariant under a unitary transformation by some unitary matrix U:

$$H' = U^T H U \tag{2.8}$$

- The elements H_{ij}, where $i \leq j$, in the matrix are all statistically independent. This means that the probability density is a product of functions that depend on one of the random variables of the matrix H. Since the variables may be real or imaginary the functions must then be separated into $H^{(re)}$ for the real variables and $H^{(im)}$ for the imaginary variables:

$$P(H) = \prod_{i \leq j} f_{ij}(H_{ij}^{(re)}) \prod_{i \leq j} f_{ij}(H_{ij}^{(im)}) \tag{2.9}$$

The GUE usually models systems with external fields, so for the GUE to be applicable to a physical system Mehta mentions that, "[...] for the unitary ensemble

to be applicable, the splitting of levels by the magnetic field must be at least as large as the averge level spacing in the absence of the magnetic field"(Mehta, 2004).

For the GUE we have the following approximate distribution function(Haake)(Mehta, 2004)(Reichl, 1992):

$$P(s) = (\frac{32s^2}{\pi^2})e^{\frac{-4s^2}{\pi}} \tag{2.10}$$

Determining Quantum Chaos

After defining the Gaussian ensembles, the biggest question that arises is: how do the random matrices allow us to characterize or determine whether a quantum system manifests chaos? Tomaž mentions that," The [...] working definition is the reference with the *random matrix theory*, namely the many-body quantum system is said to be chaotic if its excitation spectrum or some other dynamical properties can be (on certain energy, or time scale) well described by ensembles of random Hermitian matrices with appropriate symmetry properties" (Prosen, 2007)(Mehta, 2004). Additionally, spectral properties of quantum systems have that manifest chaos in the classical limit are similar to those seen in the spectra of the random matrices(Reichl, 1992).

Furthermore, Berry and Tabor proved that, "[...] the spectral spacing statistics of integrable systems exhibit Poisson-like behavior [...]"(Berry and Tabor, 1977)(Reichl, 1992).

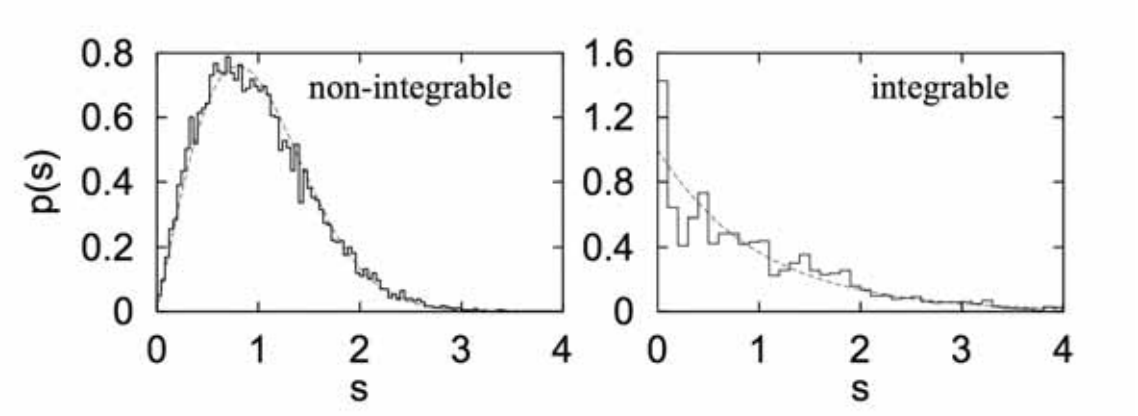

Figure 2.2: Nearest neighbor level spacing distribution for a quantum chaotic case H_C (left) and an integrable regular case H_R (right) with level spacing distributions of the GOE, Eq.(2.9), and Poisson, Eq.(2.11), respectively.(Prosen, 2007)

The connection here is with the work done by McDonald and Kaufman (Mc-

Donald and Kaufman, 1979) who studied billiards and experimentally demonstrated that classically integrable systems have Poisson-like distributions (non-chaotic system) whereas the classically chaotic system presented a Wigner-like distribution. These results were analized by Bohigas, Giannoni and Schmidt (Reichl, 1992) by using the Sinai billiard and obtained the results shown in Fig (2.3) and have been reviewed and proven once more by Prosen (Prosen, 2007) as shown in Fig (2.2). Because of these results we must then also compare the results to the Poisson distribution in order to better determine whether the system manifests or not chaos and is given by

$$P(s) = e^{-\lambda}\frac{\lambda^s}{s!}. \tag{2.11}$$

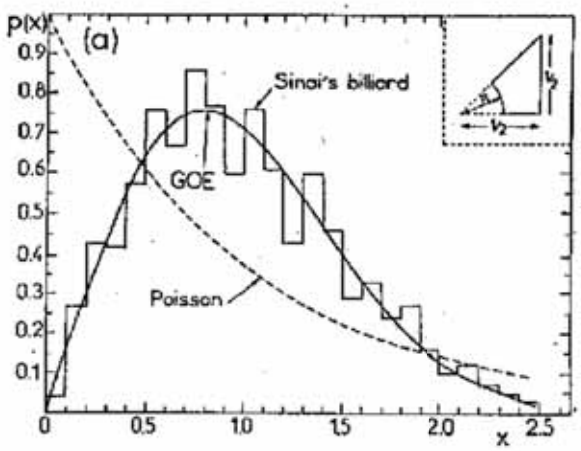

Figure 2.3: Histogram of energy level spacings of Sinai's billiard. The dotted line is the Poisson approximation and the solid line is the Wigner-like approximation using the GOE ensemble. (Weidenmuller and Mitchell, 2009)

Ultimately, the integrability of a quantum system determines whether it manifests chaos or not but we will not be focusing on integrability but rather on whether the electronic structure manifests or not chaos. In order to do this we will compare the Poisson-like, GOE (Wigner-like) and GUE distributions to the level spacing distribution (LSD) and see which one fits best.

2.2 Density Functional Theory (DFT)

2.2.1 Introduciton to DFT

Many-body Hamiltonian of the electron gas

DFT stands for Density Functional Theory and is usually the *ab initio* theory for molecules and solids by analyzing the *electron gas*,"[...] a set of interacting point electrons moving quantum-mechanically in the potential field of a set of atomic nuclei, which are considered to be static"(Argaman and Makov). DFT is mostly used in quantum chemistry, solid state physics and condensed matter physics and is a computational method used in the many-body problem within crytalline structures with billions upon billions of molecules or atoms (usually in the range of Avogadro's number of 10^{23} in a normal sample). In order to understand its importance in the field we must first look at quantum theory and its approach to many-body physics.

In quantum mechanics there are two different approaches taken in order to understand quantum systems. Physicist Schrödinger came up with the first, and most widely used, which deals with his famous "Scrhödinger equation" whereas Heisenberg came up with the second approach. Schrödinger's approach deals with solving his differential equations while the Heisenberg approach deals more with compatible operators and various eigenfunctions. The approach we will use is Schrödinger's, and because of this we first take a look at his differential equation:

$$\hat{H}\Psi = E\Psi \tag{2.12}$$

where $\hat{H}$ is the Hamiltonian specific to the system, Ψ is the wavefunction or state and E is the Energy of the system. As can clearly be seen, Ψ is an eigenfunction and E is its eigenvalue when operated by the Hamiltonian of the system. To further understand this, the Hamiltonian of a conservative system can always be written more explicitly as the sum of the kinetic and potential energies and only depends of the momenta and positions of the objects/particles in the system:

$$H(p, \vec{x}) = T(p) + U(x) \tag{2.13}$$

$$H(p, \vec{x}) = \frac{p^2}{2m} + U(x) \tag{2.14}$$

$U(x)$ is always defined by the system's potentials but the kinetic energy can

generally be defined as in 2.14.

It is especially important to notice that the potential and kinetic energies have a specific dependence in variables as this affects many of the assumptions and simplifications made for these conservative systems and the way the Hamiltonian itself is being written in this way. While there may be, for example, potentials that are dependent in the momentum of a particle, the simple electronic systems being dealt with do not behave this way and thus do not have any U depedent of p. The Schrödinger equation can be extended for many bodies.

The extension of the wavefunction to many bodies is the dependence on all of the bodies being studied. This can then we written in the following manner:

$$\Psi = \Psi(\vec{r}_1, \vec{r}_2, ..., \vec{R}_1, \vec{R}_2, ...) \tag{2.15}$$

where the $\vec{r}_i$ are the position vectors of the electrons and the $\vec{R}_i$ are the ones for the atomic nuclei. Thus the many-body equation would be written as:

$$\hat{H}\Psi(\vec{r}_1, \vec{r}_2, ..., \vec{R}_1, \vec{R}_2, ...) = \epsilon_N \Psi(\vec{r}_1, \vec{r}_2, ..., \vec{R}_1, \vec{R}_2, ...) \tag{2.16}$$

in which we now take into account all the electrons or nuclei of the system. Treating a N-body electron gas we may now write the Hamiltonian more generally:

$$H(\hat{p}, \vec{x}) = T(\hat{p}) + U(\hat{x}) + V(\hat{r})$$

$$H(\hat{p}, \hat{\vec{x}}) = \sum_i^N \frac{\hat{p}_i^2}{2m_i} + U(x) + V(\hat{r}) \tag{2.17}$$

here the additional term V is the two-particle interaction. We may write the kinetic energy more explicitly because in quantum mechanics quantization of the momentum operator results in $-i\hbar\nabla$ when dealing with a three-dimensional system.

Born-Oppenheimer Approximation

We may now approach the electron gas problem for molecules and solids. Since DFT is a theory that deals with electron densities, we must be able to separate the nuclear energies from the electronic energies. The Born-Oppenheimer approximation states two things:

- The nuclei move much slower than the electrons ($v_{e^-} \gg v_{nuclei}$) and thus one

can say their kinetic energies are zero in comparison, and that the total state of the system

- The motion of nuclei and electrons (the wavefunction Ψ) can be separated and written as a product of the two: $\Psi_{tot} = \psi_{e^-} \times \psi_{nuclei}$

First, we'll write the Hamiltonian without the approximation and then with the separation.

Since the Hamiltonian must take into account the kinetic and potential energies of all the bodies as well as the electromagnetic interactions between the particles and nuclei, we use Coulomb's law to describe such interactions as well as the usual kinetic energies.

We then obtain the general Hamiltonian for the electron gas:

$$\hat{H} = -\frac{\hbar^2}{2}\left[\sum_i^N \frac{\nabla^2_{\vec{R}_i}}{M_i} + \sum_i^N \frac{\nabla^2_{\vec{r}_i}}{m_e}\right]$$
$$-\frac{1}{8\pi\varepsilon_0}\left[2\sum_{i,j}\frac{e^2 Z_i}{\left|\vec{R}_i - \vec{r}_j\right|} - \sum_{i\neq j}\frac{e^2}{|\vec{r}_i - \vec{r}_j|} - \sum_{i,j}\frac{e^2 Z_i Z_j}{\left|\vec{R}_i - \vec{R}_j\right|}\right] \tag{2.18}$$

in which the M_i are the nuclei masses, Z_i the atomic numbers of the i-th nucleus, m_e is the electronic mass, and e is the Coulombic charge equal to $1.6 \times 10^(-19)J$.

Applying the Born-Oppenheimer approximation we get the following Hamiltonian:

$$\hat{H} = \hat{H}_{e^-} + \hat{H}_{nuclei}$$

and thus

$$\hat{H} = \left[-\frac{\hbar^2}{2}\sum_i^N \frac{\nabla^2_{\vec{r}_i}}{m_e} - \frac{1}{8\pi\varepsilon_0}\left(2\sum_{i,j}^N \frac{e^2 Z_i}{\left|\vec{R}_i - \vec{r}_j\right|} - \sum_{i\neq j}^N \frac{e^2}{|\vec{r}_i - \vec{r}_j|}\right)\right]$$
$$+\left[-\frac{\hbar^2}{2}\sum_i^N \frac{\nabla^2_{\vec{R}_i}}{M_i} - \frac{1}{8\pi\varepsilon_0}\sum_{i,j}^N \frac{e^2 Z_i Z_j}{\left|\vec{R}_i - \vec{R}_j\right|}\right] \tag{2.19}$$

As can be seen, the Hamiltonian 2.18 is much more complex than that of equation 2.14 or even 2.17 and because of this complexity the energy eigenvalues for the Schrödinger equation become impossible to determine exactly and so must be

approximated with numerical techniques. One of the most powerful and computationally simple techniques is DFT. DFT can be divided into two subjects of utmost importance: Hohenberg-Kohn theorems and the Kohn-Sham equations. The theorems set up the theoretical backbone of DFT while the equations are the ones that will ultimately halp us obtain the approximations we require through distinct methods such as LAPW and APW+lo.

The Pauli Exclusion Principle

In order to correctly and completely describe an electron we must describe its spin. We may say that the up and down spins are determined by two different wave functions s_u and s_d. These two must then complete and orthonormal in order to have a full description of the spin:

$$\langle s_u | s_d \rangle = \langle s_d | s_u \rangle = 0$$

$$\langle s_u | s_u \rangle = \langle s_d | s_d \rangle = 1$$

The most important aspect of the spin is the following requirement: *A many electron wave function ust be antisymmetric with respect to the interchange of the coordinate $\vec{x}$ (both space and spin)of any two electrons.*(Szabo and Ostlund)

The coordinate mentioned has the following dependency:

$$\vec{x} = \{\vec{r}, \omega\}$$

Furthermore, the antisymmetry requirement tells us that:

$$\Phi(\vec{x}_1, ..., \vec{x}_i, ..., \vec{x}_j, ..., \vec{x}_N) = -\Phi(\vec{x}_1, ..., \vec{x}_j, ..., \vec{x}_i, ..., \vec{x}_N) \tag{2.20}$$

The importance of this is that two electrons cannot occupy the same space at the same time if they are in the exact same physical state. One way that this can be avoided is by changing the spin of one of the two adjacent same-state electrons in order to have a different total state of the particle.

Hohenberg-Kohn Theorems

In order to use DFT we must first look at the theoretical backbone that comprises DFT. Because DFT is used in electronic systems, then the theory used must also

be realted to such systems. The Hohenberg-Kohn theorems are related to electron gas systems that are under an external potential $V_{ext}(\vec{R})$ (the term "external" means that the potential is not from the electrons themselves but rather from the Coulomb potential created by the interaction with the nuclei(Rushton, 2002)). One of the main assumptions made in the theorems is that the ground state is nondegenerate, meaning that the state only corresponds to one measurable state. The theorems are as follow(Ocaña, 2004)(Scholl and Steckel, 2009):

H-K Theorem 1: "The ground-state energy from Schrödinger's equation is a unique functional of the electron density."

The energy in this theorem, as mentioned, is a functional that depends on the electron density and is also known as the free-energy Hohenberg-Kohn functional. Generally speaking, it can be written as

$$E_{tot}[n(\vec{r})] = F_{HK}[n(\vec{r})] + \int n(\vec{r})V_{ext}(\vec{R})d\vec{r} \tag{2.21}$$

where $F_{HK}[n(\vec{r})]$ is the Hohenberg-Kohn functional, the integral takes into account all the interactions of the electron density with some external potential, and $n(\vec{r})$ is the electron density and can be written as $n(\vec{r}) = 2\sum_i \psi_i^*(\vec{r})\psi_i(\vec{r})$ (the term inside the sum is the probability of electron i to be at position $\vec{r}$). Here we are writing the total energy as a function of the electronic density

Equation (2.21) is a direct result from the fact that the energy operator can be written as the expectation value of the Hamiltonian(Rushton, 2002)(Ocaña, 2004):

$$\langle\Psi|\,\hat{H}\,|\Psi\rangle = \langle\Psi|\,\hat{T} + \hat{V}_{int}\,|\Psi\rangle + \langle\Psi|\,\hat{V}_{ext}\,|\Psi\rangle$$

$$= E_{tot}[n(\vec{r})] \tag{2.22}$$

The most important result one can obtain from the first theorem is that *the ground-state electron density completely defines all the properties of the system.* The importance of this is the fact that in practice the previous problems had to deal with 3N dimensions (the dimensions of all N electrons had to be taken into account) from the wave but now the only thing that has to be taken into account is the ground-state electron density with three spatial coordinates. This means that the 10^{23} electrons would yield a problem with $3N \times 10^{23}$ dimensions! This would be nearly computationally impossible to achieve even with supercomputers in a realtively "decent" amount of time. On the other hand, solving a three-dimentional problem is much

simpler and quicker, making DFT a great tool that requires much less computational power.

H-K Theorem 2:"The ground-state energy can be obtained variationally: the density that minimises the total energy is the exact groundstate density."

An alternate way that this theorem is stated is the following(Scholl and Steckel, 2009): "The electron density that minimizes the energy of the overall functional is the true electron density corresponding to the full solution of the Scrödinger equation."

The importance of the second theorem is that it assures that there is a density that is minimum and that is exact, yet does not explicitly state what it is. That is the main problem that is trying to be solved currently as it would exactly determine the solution to the Schrödinger equation. These theorems do not state a way of calculating the ground-state energy.

Kohn-Sham Equations

Years later, in 1965(Ocaña, 2004), Kohn and Sham devised a way to aproximately calculate the functional in a numerical manner.

The Hohenberg-Kohn functional must take into account the specific system being dealt with and cannot be written explicitly in most cases. When working with the electron cloud the problem must then be treated in a quantum-mechanical way. To construct the functional, we take into account interacting electrons(Argaman and Makov) and then write the functional in the following way:

$$F_{HK} = F_{ni}[n(\vec{r})] + E_{es}[n(\vec{r})] + E_{XC}[n(\vec{r})] \tag{2.23}$$

where $F_{ni}[n(\vec{r})]$ is the "non-interacting" term dependent on the kinetic enregies, $E_{es}[n(\vec{r})]$ is the term that includes the eletrostatic interactions, and $E_{XC}[n(\vec{r})]$ is the exchange-correlation energy.

In general there are interacting and non-interacting parts, or functions, of the free-energy functional. As mentioned by Argaman(Argaman and Makov), knowledge of the system would allow to construct the first term but is not necessarily an easy task. On the other hand, the exchange-correlation energy includes "everything else" which means that it includes all of the many-body physics and possible interactions which makes its explicit form unknown. The equations that arose from this analytical approach are called the Kohn-Sham Equations and are the main approach to the problem.

A very common approximation used for the many-electron problem is the Local

Spin Density Approximation (LSDA)(Blaha et al.). This approach was used by Kohn and Sham in which they showed that the solution was self-consistent in an iterative process. The Kohn-Sham equations have the following general form:

$$\left[-\frac{\hbar^2}{2m}\nabla^2 + V(\vec{r}) + V_H(\vec{r}) + V_{XC}(\vec{r})\right]\psi_i(\vec{r}) = \epsilon_i\psi_i(\vec{r}) \tag{2.24}$$

The solutions to these equations are single-electron wave-functions that depend only on the three spatial variables of the electronic density. As mentioned before, the N-dimentional problem was reduced to a 3-dimensional problem, which greatly facilitates the computational power required. On the left-hand side of the equation, the potential V is the same as in the Hamiltonian from equation (2.17) and describes the interactions between the electron i and the atomic nuclei. The potential V_H is the Hartree potential(Scholl and Steckel, 2009) and is defined as

$$V_H(\vec{r}) = e^2 \int \frac{n(\vec{r})}{|\vec{r} - \vec{r}'|} d^3r' \tag{2.25}$$

and describes the electron repulsion between the electrons considered and the electronic density of all the electrons. Additionally, it includes a term known as a "self-interaction" term because the electron itself being considered is part of the total electron density. Ultimately, this means that part of the Hartree potential includes a term in which the electron interacts with itself. Because this has no real meaning, the model itself must correct this term. In fact, all corrections made to the model are included within the last of the terms, the V_{XC} potential.

Finally, the potential V_{XC} is the exchange-correlation potential. As the name suggests, the potential takes into account any exchange and correlation contributions. We can define this potential in terms of the exchange-correlation energy mentioned previously in equation (2.23):

$$V_{XC} = \frac{\delta E_{XC}(\vec{r})}{\delta n(\vec{r})} \tag{2.26}$$

The importance of this is that we can now create a self-consistent process that will approximate the ground-state electron density. Computationally what happens is the following:

- first we define an initial electron density $n1(\vec{r})$
- then obtain the solutions to the Kohn-Sham equations

- calculate a second electron density function from the solutions obtained previously and compare to the first one. If the densities are equal then it is the ground-state energy. Otherwise, the first density must be modified in order to try and obtain equal or closer values. This proces is repeated until the difference between the two is equal to or smaller than some accepted error or the two are equal.

2.2.2 Approximations to the Correlation Function

Obtaining the correlation function is the main task of DFT and has many models which try to approximate it. We will treat the following: LAPW, APW+lo and the famous DFT+U. The advantage that these methods have is that they are self-consistent, something we need to solve the Kohn-Sham equations.

LAPW

The linearized augmented plan wave method (LAPW) is extremely accurate in electronic structure calculations. It is based on the treatment of exchange and correlation and uses the LSDA.

As stated by the Wien2k manual, "the LAPW method is a procedure for solving the Kohn-Sham equations for the ground state density, total energy, and (Kohn-Sham) eigenvalues (energy bands) of a many-electron system"(Blaha et al.).

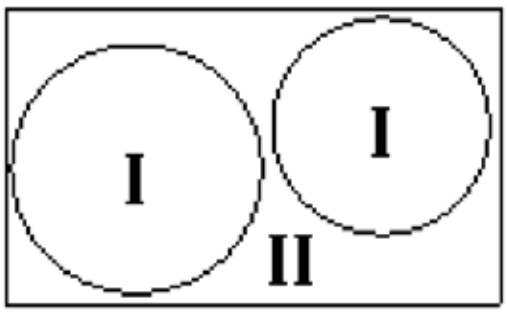

Figure 2.4: Figure showing the partition of the areas treated: atomic regions (I) and interstitial region (II). Image obtained from the Wien2k User's Manual (Blaha et al.)

To achieve this the model partitions the crystal lattice into two distinct entities: atomic spheres and interstitial regions where we can assume there is nothing. The following is done to each of the regions.

Generally, the solutions of the Kohn-Sham equations are written in the following manner:

$$\psi_{\vec{k}_n} = \sum_n c_n \phi_{\vec{k}_n} \tag{2.27}$$

where the $\phi_{\vec{k}_n}$ are the functions used to approximate in each specific region and the coefficients c_n are determined by the Reyleigh-Ritz variational principle.

As seen in figure (2.4), region (I) is the atomic sphere whose basis set is a linear combination of radial functions times spherical harmonics $Y_{lm}(\theta, \varphi)$:

$$\phi_{\vec{k}_n} = \sum_{lm} \left[A_{lm,\vec{k}_n} u_l(r, E_l) + B_{lm,\vec{k}_n} \dot{u}_l(r, E_l) \right] Y_{lm}(\theta, \varphi) \tag{2.28}$$

Here the $u_l(r, E_l)$ is the regular radial solution to the Schrödinger equation for some given energy E_l, $\dot{u}_l(r, E_l)$ is the energy derivative of the u_l in the same energy E_l. The linear combination of the two terms and their respective coefficients is what linearizes the radial function. Additionally, the coefficients A_{lm} and B_{lm} are determined by having the basis function in (I) match the plane waves with the basis function of the interstitial region (II).

In region II the function used is a plane wave expansion

$$\phi_{\vec{k}_n} = \frac{1}{\sqrt{\omega}} e^{i\vec{k}_n \cdot \vec{r}} \tag{2.29}$$

In both functions $\vec{k} = \vec{k} + \vec{K}_n$ where $\vec{k}$ is the wavevector inside the first Brillouin zone and the $\vec{K}_n$ are the reciprocal lattice vectors.

APW+lo

While the LAPW method is quite accurate, it *can* be improved. One way is to improve the linearization by adding extra basis functions that are not dependent on the $\vec{k}_n$. These new terms are known as the "Local Orbitals"(Blaha et al.) and usually consist of two radial functions at two different energies and an energy derivative as done previously:

$$\phi_{lm}^{LO} = \left[A_{lm} u_l(r, E_{1,l}) + B_{lm} \dot{u}_l(r, E_{1,l}) + C_{lm} u_l(r, E_{2,l}) \right] Y_{lm}(\hat{r}) \tag{2.30}$$

These coefficients are obtained by normalizing ϕ_{lm}^{LO} and by giving it boundary conditions between I and II equal to zero ($\phi_{lm}^{LO} = \dot{\phi}_{lm}^{LO} = 0$).

This approach can be improved, as demonstrated by Sjöstedt, Noström and Singh(Sjöstedt et al., 2000), by instead using the standard APW basis but with only the radial function and the added local orbital terms. The biggest difference is that the coefficients no longer depend on the $\vec{k}_n$ and are determined by the boundary conditions at the sphere of *lo* and that it be normalized. This in turn makes reduces the basis sets and ultimately the computational time required.

Hubbard's U-Parameter

Since the problem we are dealing with treats rare-Earth metals, specifically Lanthanides, that means that the valence shell is composed of f-orbital electrons. This is important because the on-site Coulomb interactions are stong for d- and f-orbital electrons(DFT, 2018a).

The LSDA is an approximation that uses averages of the electron interactions because it takes into account electron delocalization and one can say that over the entire crystal the interactions are overall the same. Highly correlated systems (systems that are heavy-fermi or, more clearly, materials, molecules or crystalline structures with atoms that have valence electrons usually in the 4f and 5f) the are usually localized-electron systems however, so having to average the electron interactions would be counter-intuitive since the approximation would be further off. To account for this corrections are made with additional parameters. Specifically, for strong on-site Coulomb interactions a very common parameter to use is Hubbard's U-Parameter. The correction is done on the energy of the system. The standard DFT energy is separate from the added parameter and so the new energy is written as follows:

$$E_{DFT+U} = E_{DFT} + \sum_a \frac{U_{eff}}{2} Tr(\rho^a - \rho^a \rho^a) \tag{2.31}$$

where ρ^a is the atomic orbital occupation matrix and $U_{eff} = J - U$. J and U are the exchange and Coulomb on-site parameters respectively and so the U_{eff} term accounts for the Coulomb interactions in the system.

Chapter 3

Results

3.1 DFT

The electronic systems that will be analized are the Silicon electronic structure, since it is has already been done within literature, and the electronic structure of Europium. The importance of using Lanthanides is that they are a group of elements whose Valence shell is the f orbital. As mentioned previously, it has been noticed(Liechtenstein et al., 1995) that on-site Coulomb interactions are strong for d and f electrons (electrons in d or f orbitals). Therefore, Lanthanides all present strong on-site Coulomb interactions which means we must use Hubbard's U parameter in order to improve the results.

To demonstrate the difference this parameter makes, two distinct calculations have been done, one with $U = 0$ and another with $U = 4$. These two results are compared through the band structures and how they differ as well as how the band spacing distributions change when the parameter is added.

3.1.1 Electronic Structures of Si and Eu

To be able to deal with the problem at hand, it is necessary to use the underlying symmetry manifested in the periodicity of the crystal itself. Because we are working with crystals it means that we are dealing with a many-body problem which would make it rather hard to calculate its properties because the amount of data would be unrealistic to calculate in a lifetime (somewhere near or past Avogadro's number, around 6.02×10^{23}). Since crystals are periodic we then look at the unit cell, also known as primitive or basic cells: the smallest repeating component of the crystal. Because of the difference in size, the interactions between the various elements,

and the shapes of the atoms, each unit cell is different and depends on the crystal structure.

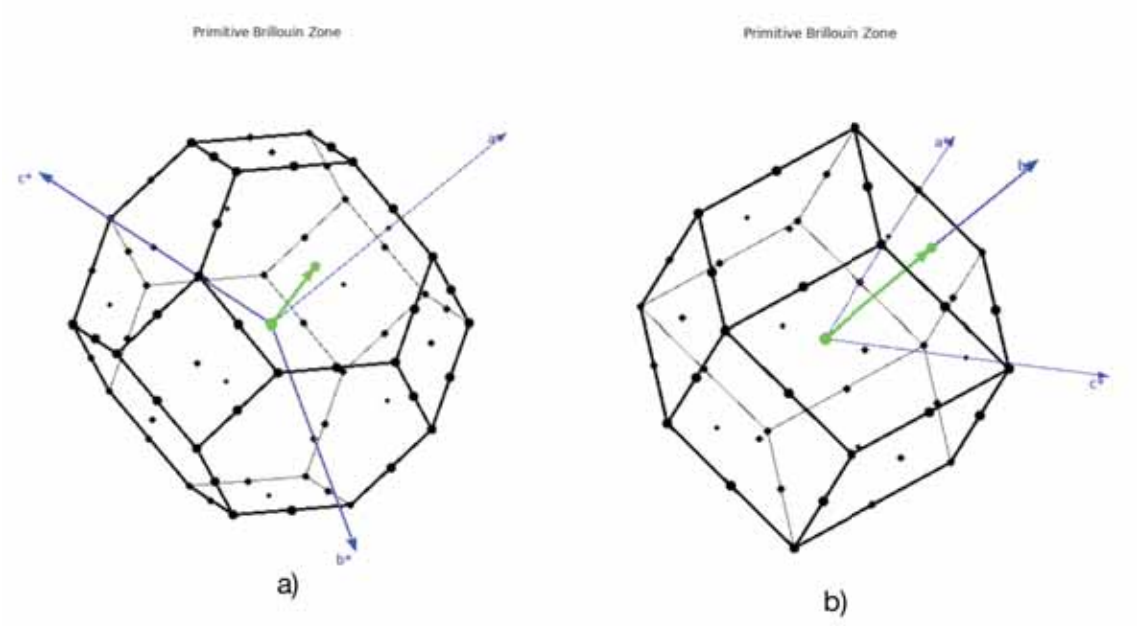

Figure 3.1: First Brillouin zone of a) Si and b) Eu calculated with the XCrysDen program. The arrow shows the direction from Γ to L for Si and from Γ to N for Eu of the Brillouin zone.

While there are many ways of defining these basic cells one of the most useful is that of the Brillouin zone as it uses the reciprocal space of the crystal in order to simplify calculations. It is defined as "a particular choice of the unit cell of the reciprocal lattice"(Chapuis, 2017a) that has to do with the Bragg planes of the crystal. The crystal structure of Si is a body-centered cubic, which according to the International Union of Crystallography (Chapuis, 2017b) has a Brillouin zone shaped as a cuboctahedron whereas the Eu crystal structure is face-centered cubic as shown in Figure B.11 and has a Brillouin zone shaped as a rhomb-dodecahedron. Figure 3.1a) shows the Brillouin zone of Si and, as stated previously, shows that it does actually have a cuboctahedron shape. The green vector represented is the path taken from Γ to L. The unit cell for Eu is body-centered cubic(EuO, 2018) as shown in Figure B.12 and the Brillouin zone for Eu, shown in Figure 3.1b), is a rhomb-dodecahedron, vastly different from the cuboctahedron. This means that the symmetry points are all different but ultimately the analysis is similar. As shown with the green vector, the symmetry we'll work with is that from Γ to one of the square faces which is denoted as N in the band structure.

The complete band structure of Si is shown in Figure 3.2. The letters on the x-axis are the symmetry points for the k-vectors.

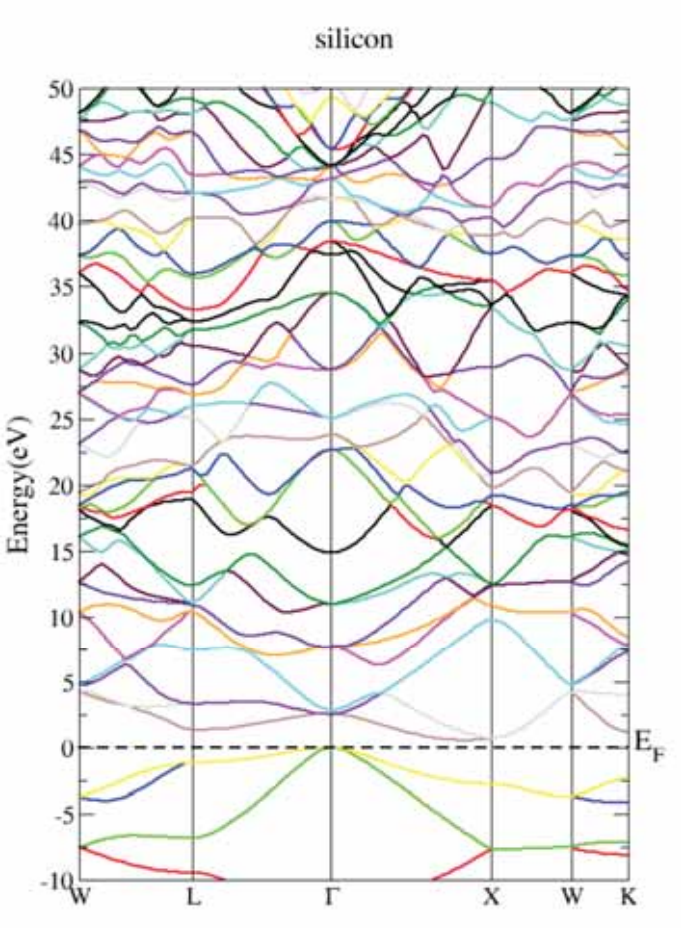

Figure 3.2: Band structure of 151 high-energy bands of Si calculated with the Wien2k program.

The complete band structure of Si is shown in Figure 3.2 and shows all symmetry points of the Brillouin zone of the crystal. It is important to note that the bandwidths below the Fermi level are large, especially compared to those above the Fermi level. Near the Γ symmetry point most bands seem to get closer to the Fermi level and then separate when away from it. Mucciolo(Mucciolo et al., 1994) calculated the band structure of Si for 90 energy bands (Figure 3.3a)). The band structures calculated with the Wien2k program (Figure 3.3 b)) are similar to those presented by Mucciolo et al. which means that our calculations done with Wien2k are quite accurate and comparable to those seen in literature. All our calculations from Γ to any symmetry point in the Brillouin zone were performed with 101 k-vectors along the path.

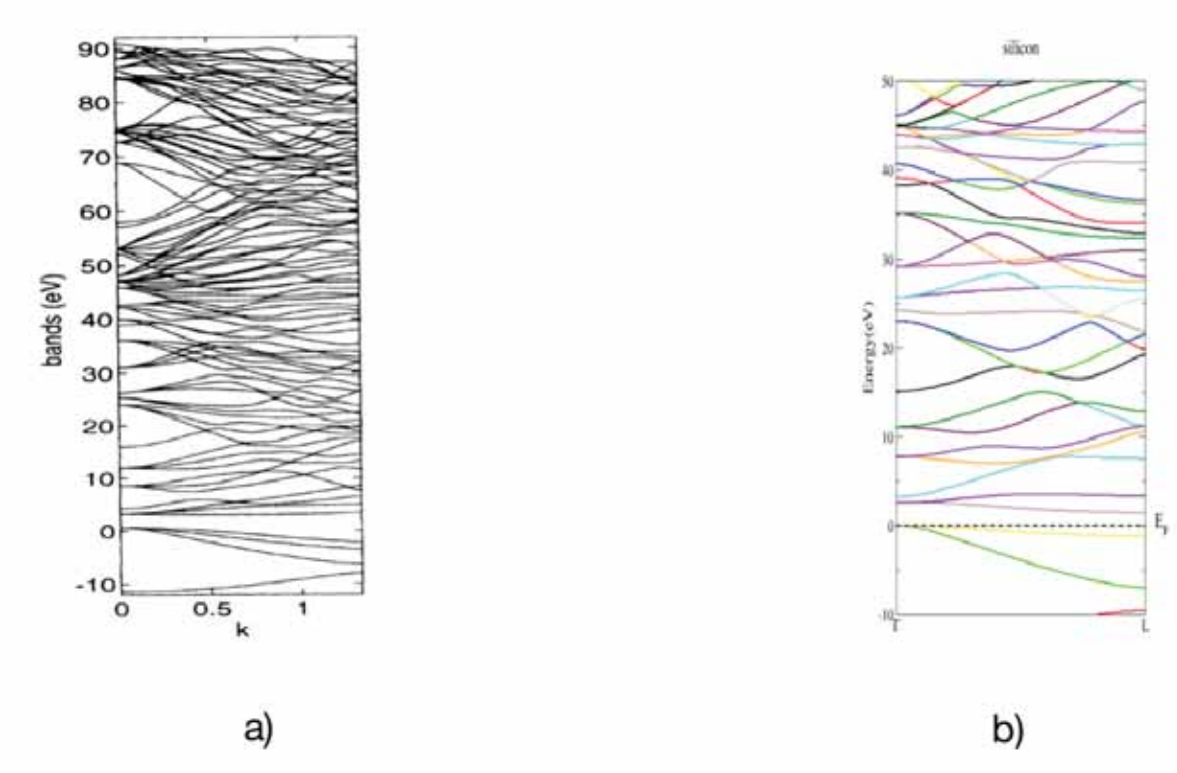

Figure 3.3: a)Band structure calculated by Mucciolo, and b) Band structure calculated with the Wien2k program from Γ to L.

Figure 3.3b) presents the band structure specifically in the region being analyzed and, as with Mucciolo, this region is the one that passes through the center of mass of the unit cell. Although they do not explicitly state which region was used, the region from Γ to L has a very similar band structure by looking at the band characteristics near Γ around 30eV and 50eV, and those near L around the E_F. For example, the bandgap between -10 and 0 eV near L is the same one as well as the gap near Γ from 15 to 23 eV and also the bandgaps around -5eV and the Fermi level. Since the DFT results for Si are very similar to those obtained by Mucciolo we can say that the band spacing distributions must manifest chaos when away from the symmetry points such as Γ and L. More importantly this allows us to look further into Eu's crystal structure knowing that the calculations are accurate.

The complete band structure of Eu is shown in Figures 3.4a) and b). Although subtle, the changes made by the U parameter can be noticed. For example, comparing Figures 3.4a) and 3.4b) near N and around E_F there are more band separations when $U = 4$. Another example is when comparing the bands near Γ around 20eV where a band appears when $U = 0$ yet does not appear when $U = 4$. While the

corrections may seem small, they are of utmost importance because the affect the entire band spacing distribution directly. Some of these important changes can be seen such as the peak in the H symmetry of Figure 3.4a) around 5eV which do not appear in Figure 3.4b). Another discrepancy between the two is another peak that appears in 3.4a) near the symmetry P and also around 5eV energy.

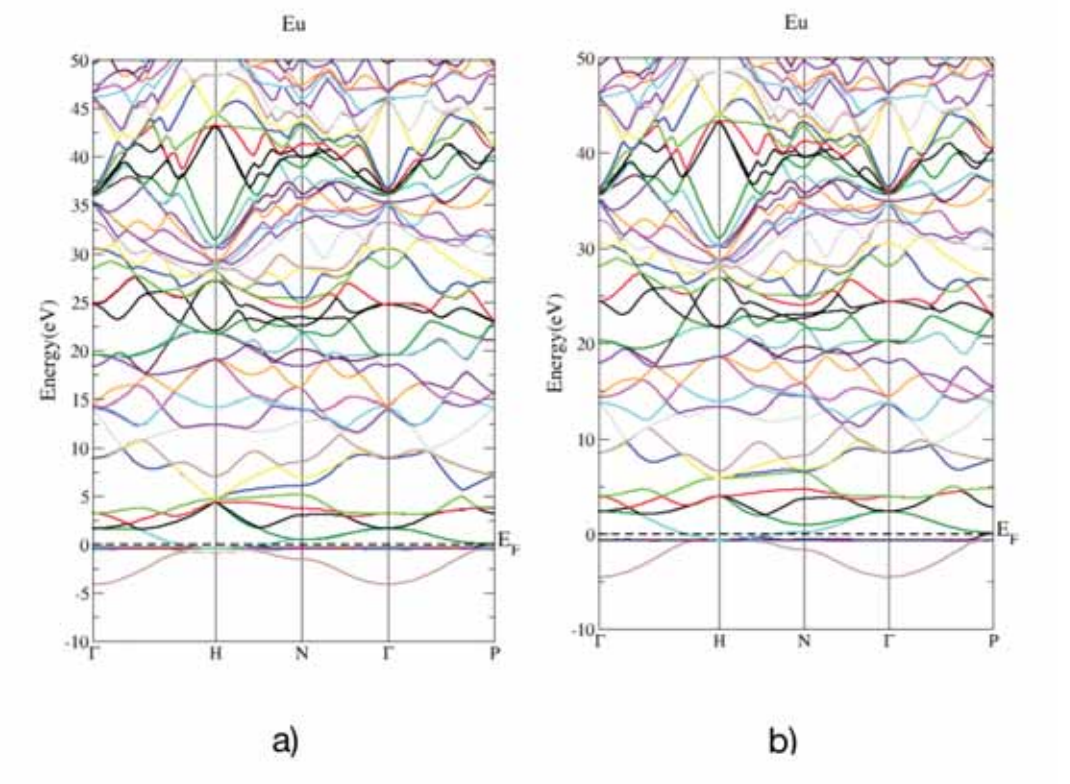

Figure 3.4: Complete band structure of Eu for a) 77 high-energy bands and $U = 0$ and b) 127 high-energy bands and $U = 4$ calculated with Wien2k.

It is important to note that the symmetry points being studied for Eu are because of the similarity with those of Si. Further analysis into Eu would require looking at symmetries where more metallic properties could be studied in-depth such as points N to H or Γ to H where bands cross the E_F (Figure 3.2). That is, the symmetry interval where the metallic character of Eu is present are N-H and L-H and the semiconductor bandgap for Si can be observed at Γ-L and Γ-X. Significant band structures are presented in Appendix B as part of the DFT calculations.

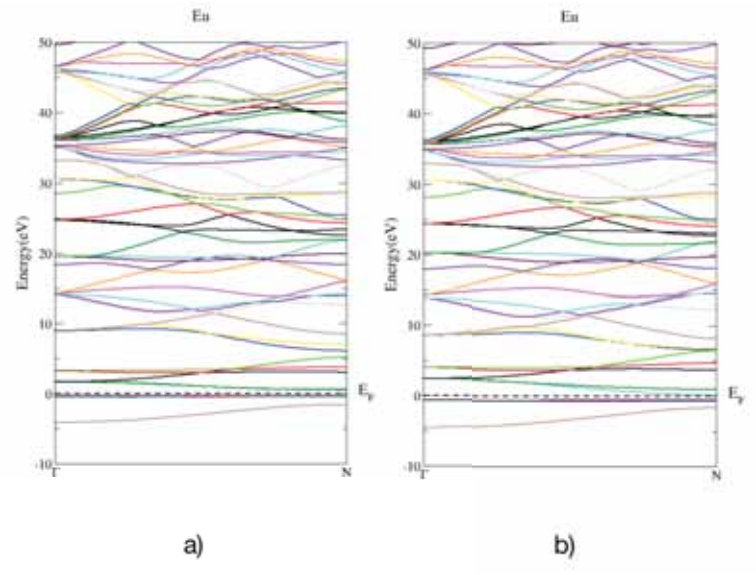

Figure 3.5: Band structure of Eu for a) 77 high-energy bands from Γ to N and $U = 0$ b) 127 high-energy bands from Γ to N and $U = 4$ calculated with Wien2k.

3.2 Energy Level Spacing Distribution

Silicon

The energy level distributions and statistics were obtained with our FORTRAN code for 151 energy bands of Si and are compared to those obtained by Mucciolo(Mucciolo et al., 1994) for 90 energy bands that manifested quantum chaology. Figure 3.6 shows the energy level spacing distribution of Si when studying the k-vectors away from the symmetry point Γ of Si as reported by Mucciolo et al. (Mucciolo et al., 1994).

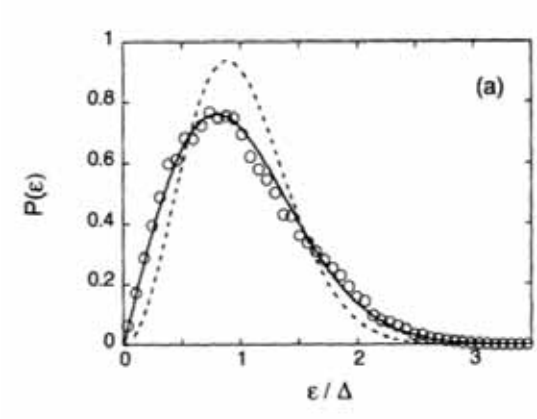

Figure 3.6: Band spacing distribution of 90 high-energy bands of Si.(Mucciolo et al., 1994)

Mucciolo et al. argue that "In order to look for quantum chaos, we have to avoid doing analysis of the spectrum at the Γ point or at any symmetry point of the Brillouin zone [...]" (Mucciolo et al., 1994) and in fact they also argue that any crystal (simple or complex) should manifest quantum chaos when analyzed away from the symmetry points this way. Figure 3.7 shows the band spacing distribution of all k-vectors that was calculated using 151 energy bands. As one can see, the distribution is similar to that of Mucciolo et al. and adjusts best to the Poisson ensemble.

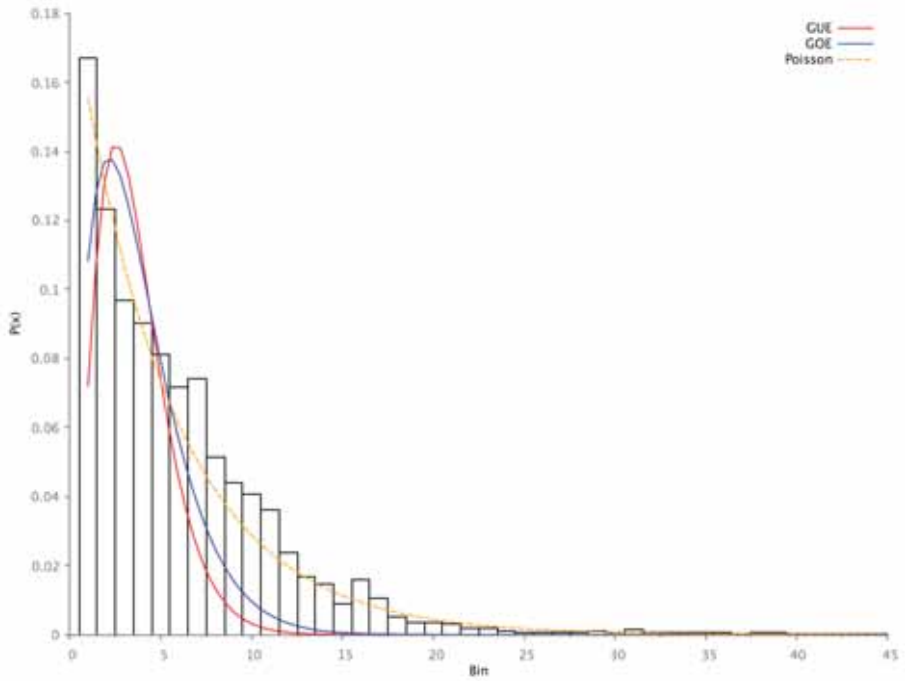

Figure 3.7: Band spacing distribution for all k-vectors of 151 energy bands of Si.

As mentioned previously, quantum chaos will manifest outside of the symmetry points. In order to visualize the transition to chaos within the electronic structure of Si, Figure 3.8 shows how the energy level spacing distribution of Si for k-vectors away from symmetry tend to manifest more and more chaos.

The energy level spacing distribution that is best approximated by the GOE is the one with k=70 of Figure 3.8 which is far away from any symmetry points. This result is consistent with those obtained by Mucciolo as well as the distributions of Hydrogen under an extermal magnetic field presented by Ghur (Ghur et al., 1997).

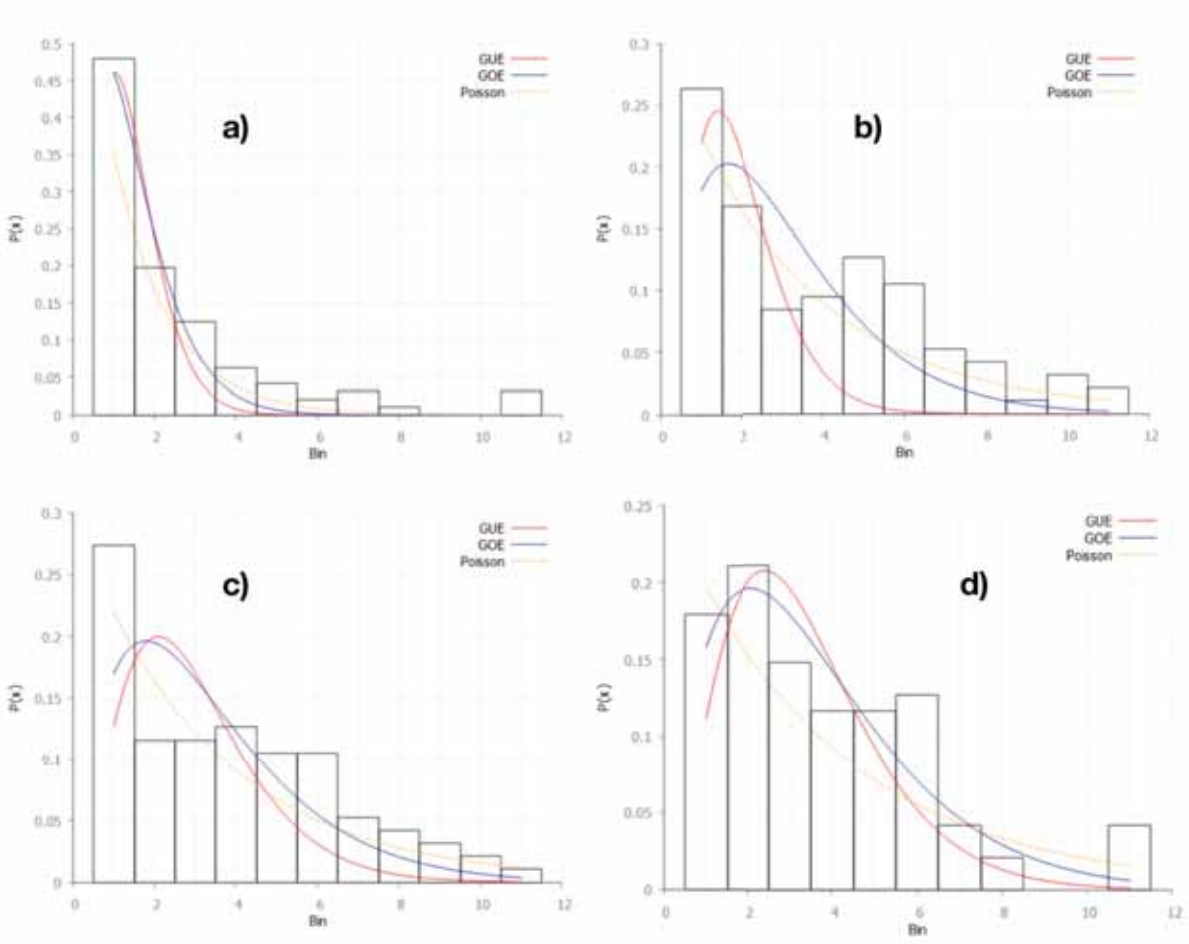

Figure 3.8: Transition to chaos for Si from Γ to L. a) k=1, b) k=30, c) k=50, c) k=70.

Europium

There are two sets of graphs for Eu: those with $U = 0$ and those with $U = 4$. The ones presented first are those that don't have the U parameter corrections for the strong on-site Coulomb interactions of the f orbital and afterwards those with the correction. Similar to the transition to chaos shown for Si, the transition to chaos made with the Eu band spacing distribution is shown for U = 0 and U = 4 in Figure 3.9 for the two most representative energy level spacing distributions.

Figure 3.9 shows the two most representative energy level distributions for Eu with U = 0 (a) and b)) and U = 4 (c) and d)).

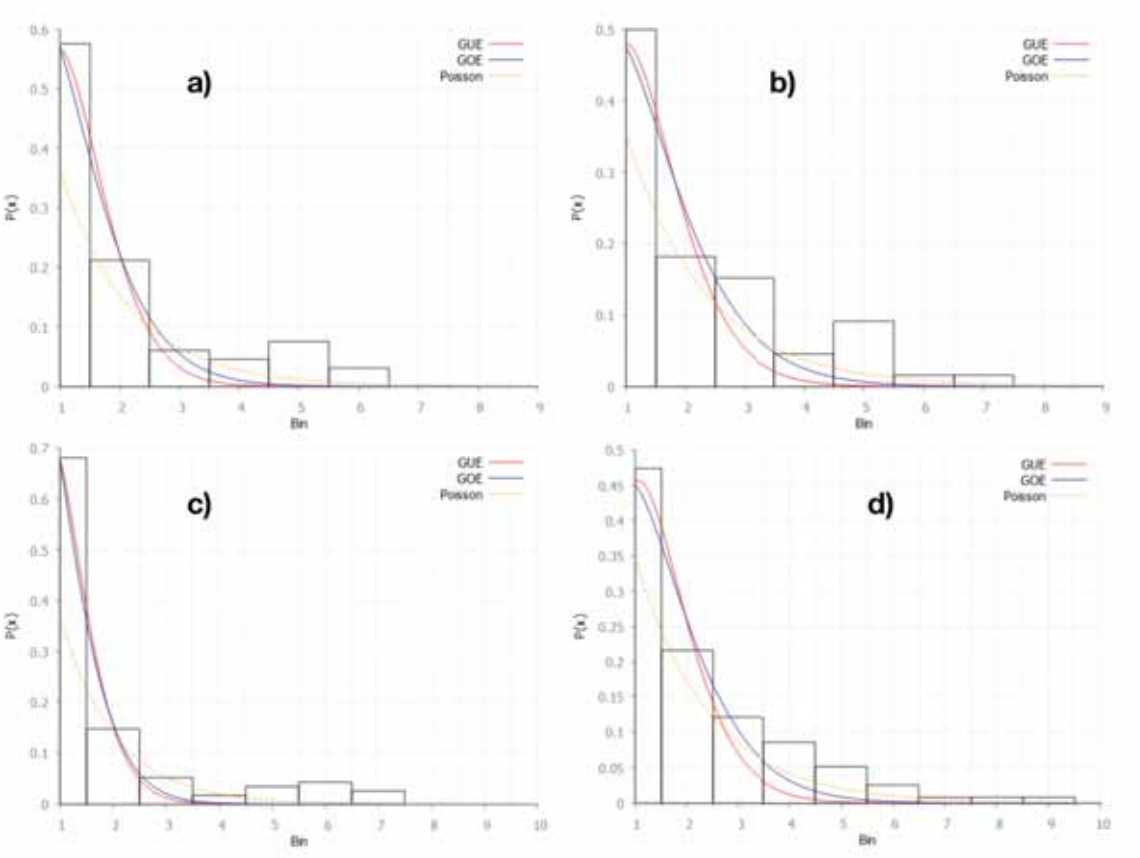

Figure 3.9: The most representative graphs of the energy level spacing distributions for Eu. The graphs have the following parameters: a) U = 0 and k = 10, b) U = 0 and k = 70, c) U = 4 and k = 10, d) U = 4 and k = 70.

Figure 3.9 shows the two most representative energy level distributions for Eu with U = 0 (a) and b)) and U = 4 (c) and d)). Histograms a) and b) show the two most representative changes in the transition to chaos for U=0 yet remain Poisson-like. Similarly, histograms c) and d) are the two most representative graphs for U=4 and remain Poisson-like aswell but seems to have a smoother profile.

The same k-vectors are calculated in order to compare both series of graphs. The most noticable difference between the two sets of graphs is the fact that the distributions with U = 0 aren't as smooth or regular as those with U = 4. This could be a sign that LSDA calculations for valence orbitals that are d or f orbitals must use Hubbard's U parameter to correct the strong on-site Coulomb interactions that are present within these orbitals. Additionally, none of the graphs seem to manifest chaos, something that shouldn't happen according to Mucciolo et al., since even simple crystals should manifest chaos when analyzed away from symmetry points.

Looking at the distributions tells us that Eu doesn't seem to manifest quantum

chaos. This failure to demonstrate the chaos that must appear is due to the lack of information in the model. In other words, it needs the Hubbard parameter to account for the strong on-site interactions in order to more accurately model the band structure of Eu. A more in depth analysis which addresses how the Hubbard parameter would correct this is is required, since the entire set of obtained graphs reveals a Poisson-like shape, which contrasts the expected Wigner-like shapes according to Mucciolo.

Furtheremore, the parameters that fit the distributions help us look at which of the three best fit the histograms. We look specifically at the last graph for Eu with $U = 0$ and Eu with $U = 4$ which are the ones where chaos should manifest. The Poisson-like fit had one parameter to fit μ_p, while the GOE and GUE each had three: one for amplitude of distribution A, width of bell σ_w, and translation along axis towards the mean value μ_g. For the model with $U = 0$ the best fit was the Poisson-like fit with a parameter percent error of 32.71% whereas the GOE parameters had the following errors: A with 4657%, σ_w with 542.6%, μ_g with an 643.7% error. The GUE had the following percent errors: A with 7464%, σ_w with 629.4%, μ_g with an 758.3% error. On the other hand, the Eu model with $U = 4$ also best fit with the Poisson-like distribution with the a parameter percent error of 33.51%. The percent errors of the GOE are as follow : A with 1960%, σ_w with 318%, μ_g with an 401% error. The GUE had the following errors: A with 5377%, σ_w with 460%, μ_g with an 556.7% error. From these parameters one can notice that between the GOE and GUE distributions the better fit is the GOE which would seem that with better approximations to the model that account for the strong on-site interactions could then manifest chaos.

The distribution for all the k-vectors of each model is shown in Figure 3.10. Both present a Poisson-like distribution as expected (due to the inclusion of the symmetry points) but the largest difference between the two is the first bin. For the model with $U = 0$eV we have many more zeroes (a probability of around 0.42) than the model with the on-site corrections (a probability of around 0.26). This ultimately makes a smoother Poisson distribution for the corrected model. Comparing their paramter fits for the Poisson-like distribution, the non-corrected model had a percent error of 38.56% whereas the corrected model has a percent error of 29.9% which suggests that it has a smoother distributionand that an increase of the Hubbard parameter could also lead to manifestation of chas for the same value of the k-vector.

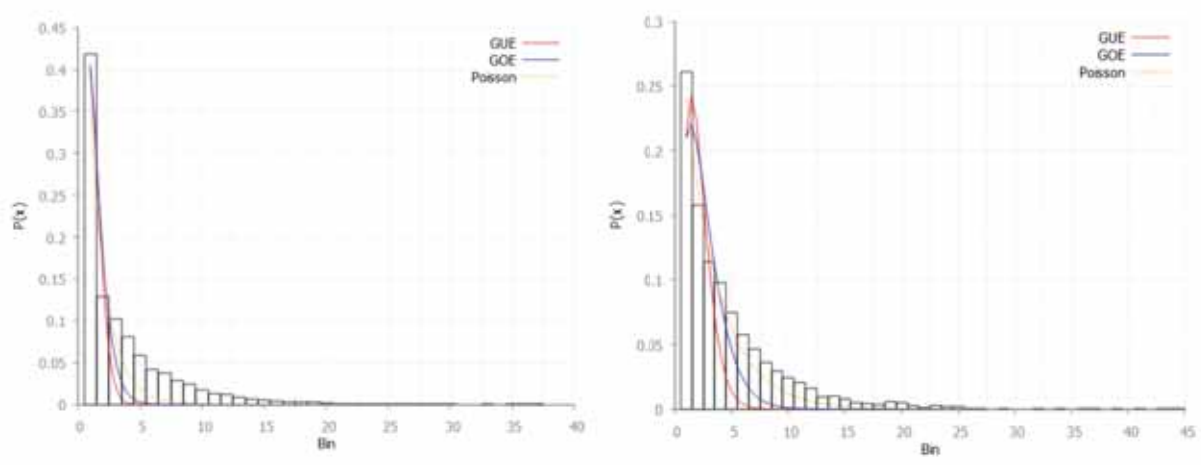

Figure 3.10: Band spacing distributions for all the k-vectors of 77 energy bands of Eu with $U = 0$eV (left) and 127 energy band of Eu with $U = 4$eV (right).

Ultimately, this means that Mucciolo's approach does not apply at all for electronic structures with strong on-site interactions in their valence shells such as the Lanthanides. Additionally, other possible factors contributing to this could be the conductivity of the metal and as such the symmetries in the band structure containing this information should also be compared. More complete energy level spacing distribution transitions for Eu and Si are presented in Appendix B.

3.3 Velocity Distribution

The velocity distributions of the band structure k-vectors gives us additional information of the band structure of Si and Eu near the Fermi energy of each crystal. One of the most perplexing finds was that Eu doesn't seem to manifest chaos as Si does.

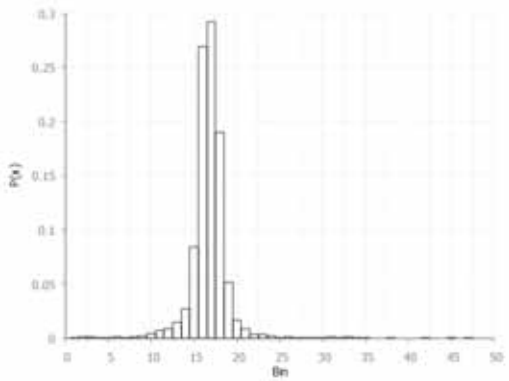

Figure 3.11: Velocity distribution of the Si k-vectors.

The Si velocity distribution of Figure 3.11 shows a gaussian distribution behavior around the bin 17 which includes the zero velocity. It has a maximum value of 0.2924 while the range of in which the most prbable valocities are in the range of $v_i - v_f$. It also has a larger bandwidth than those of Eu (Figures 3.12a) and 3.12b)). This spread is easily seen in the band structure of Si in Figure 3.2 in which all the bands below the Fermi level have a larger bandwidth. On the other hand, the bands below the Fermi level of Eu are not spread out but rather quite the opposite as shown in Figure 3.11.

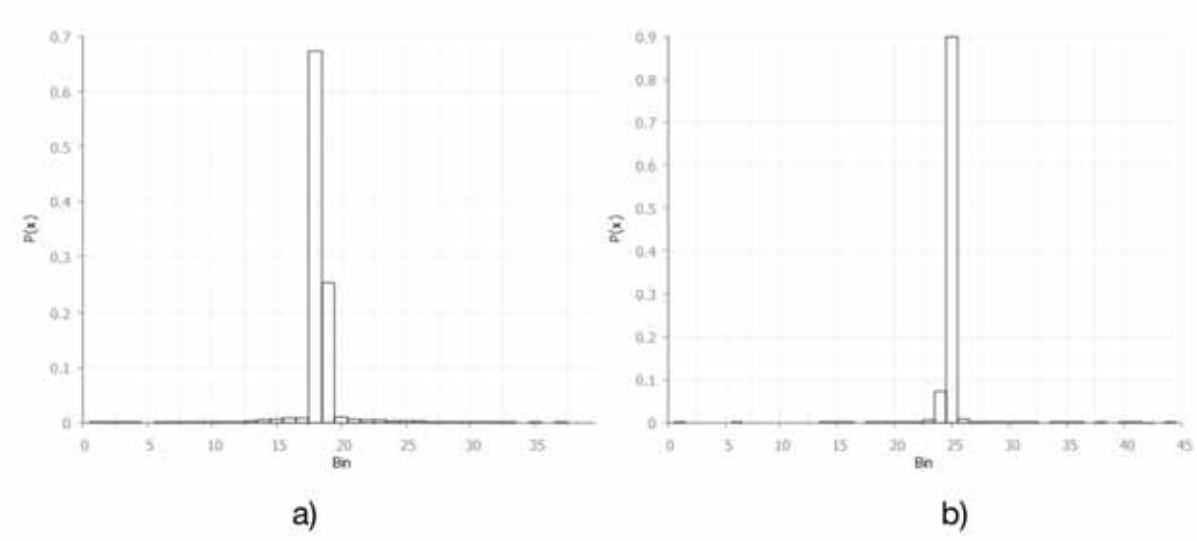

Figure 3.12: Velocity distribution of the Eu k-vectors for a) $U = 0$ and b) $U = 4$.

The distributions of Figure 3.12 show a high concentration around the zero (looks like a dirac delta function) which means that most of the band concentrated around the Fermi energy are "flat" bands. By looking at the band structure of Eu this becomes apparent, especially when we look at the flat bands near the Fermi energy that are more apparent (Figure 3.13). When comparing the Si and Eu band structures this important feature at first glance isn't noticable, yet becomes remarkably important when analyzing not only the band spacing distributions but also the velocity distributions. This important piece of information can then help us conclude that the strong on-site interactions present in the f and d orbitals of Eu play a big role in hiding the quantum chaos that the crystal should transition towards.

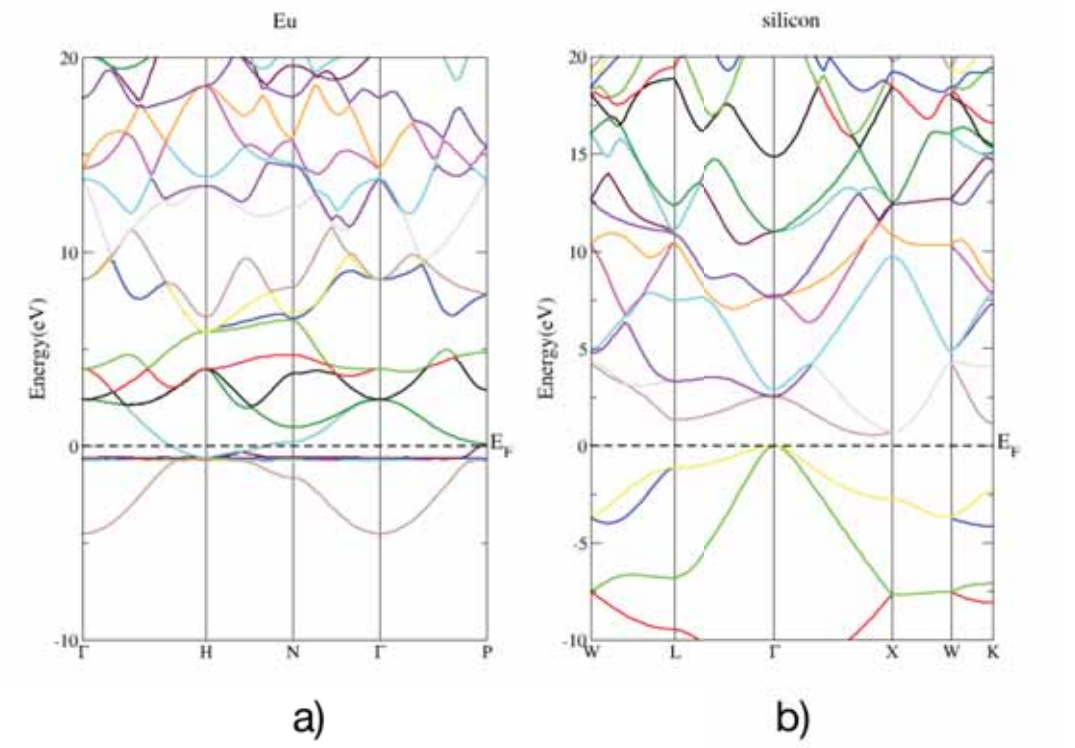

Figure 3.13: Complete band structure of a) Eu with U = 4 for 127 high-energy bands around the Fermi level, and b) Si for 151 high-energy bands around the Fermi level.

While the two velocity distributions seem similar, the differences in concentration are due to the corrections done by the U parameter. The velocity distribution of the corrected model shows a probability of around 0.9 for velocities around zero and less than 0.1 distributed elsewhere. Comparatively the distributions for the non-corrected model show that the highest proability, also centered around zero, is around 0.7. This is a big difference statistically and tells us that many of the bands that may be separate in the uncorrected structure are actually not as separate, or the separation is reduced due to the effect of correlation.

Chapter 4

Conclusions

The previous work done on Si by Mucciolo et al. (Mucciolo et al., 1994) provided a solid background in the calculations that had to be done for Si. This theoretical backbone was used to compare data and ultimately confirm whether calculations done with DFT were correct in order to use our FORTRAN code to calculate the band spacing distributions as well as the velocity distributions of Si and Eu. While the previous work proved to be right with relation to Si, it was observed that a similar approach to crystal structures does not represent the band spacing distributions when presented with stong on-site Coulomb interactions of d and f orbitals like Eu. It is well known that f and d orbitals in Lanthanides and Actinides are flat bands and energetically located around the Fermi energy. The effect of the Hubbard parameter does not affect the band spacing distribution but it does affect the velocity distribution since it flattens those bands making it more likely to obtain velocities near zero. Therefore, Mucciolo's hypothesis that any simple crystal should manifest chaos away from any points of symmetry is not completely correct for strongly correlated electronic systems such as those where f and d orbitals are relevant. Due to this, quantum chaology did not seem to manifest for Eu as hypothesized.

On the other hand, the idea of analysing transitions towards chaos provided by Ghur (Ghur et al., 1997) proved insightful in analysing how the k-vectors at points in and out of symmetry within the Brillouin zone, specifically the Γ and N points for Eu and the Γ and L points for Si affect the level spacing distributions. It was especially important in comparing the Eu models with and without the on-site interaction corrections because it was easier to notice how the Hubbard parameter affected not only the band structure but also the band spacing distributions and the velocity distributions. This eventually translated into the failure of any of Eu

distributions at portraying the manifestation of quantum chaos that should appear when analyzing points in asymmetric parts of the Brillouin zone since it seemed that the distributions were Poisson-like rather than Wigner-like.

Further work should address varying the Hubbard parameter and see exactly how this affects the band structure as well as the band spacing distributions and the velocity distributions and whether this has a very noticeable effect on the calculations or not. Ultimately this would allow us to determine if this was the main factor that did not allow the breaking of symmetries and thus manifesting chaos.

Moreover, the Hubbard parameter is not the only available model that corrects the on-site interactions and could be compared to other existing approximations. One of these approximations is known as the Hybrid potential approximation which incorporates DFT's LSDA approximation along with the Hartree-Fock approach of the exact exchange energy.

A look into the metallic portion of the band structure would provide a great insight into properties of the crystal structure such as conductivity and magnetic properties and as such would be another important task in any future research. Specifically, studying the symmetries from Γ to H or from N to H could provide information of more metallic properties of the crystal because of the bands that cross the Fermi energy.

Studying the band spacing distributions of the rest of the Lanthanides would provide a good overall insight into the statistics of these elements as well as a more in depth analysis of the electronic structure of the Lanthanide crystals.

Further analysis of the velocity distributions near the symmetry points, away from them and near the Fermi energy level could prove useful in further studies of the band structure and how the Hbubard parameter affects the overall calculations as well as how easily quantum chaos manifests within the crystal (whether it manifests it only away from the symmetry points or if it is also manifested near them).

Finally, analysis of a Lanthanide with a face-centered structure should be studied in order to directly compare the results with those of Si. This would then allow for a more in-depth comparison between the on-site interactions and the lack thereof.

Appendix A

FORTAN Code

In this apprendix the FORTRAN code used to create the band spacing distributions as well as the velocity distributions is presented.

```
program SPAGHETTI

! ---------------------------------------------------------
! ----------------------- Variables -----------------------

! Variables de SPAGHETTI data
integer*8 input_nband, input_nvectork
integer*8 nband, nvectork
real*8 d_vectork
real*8, allocatable :: levelspacing(:),velocity(:)
real*8, allocatable :: delta_ls(:)
integer*8, allocatable :: Dist_LS(:),Dist_V(:)
real*8, allocatable :: energy(:,:), totalenergy(:,:)

!General variables 2
real*8 rtrash
real*8 beta
integer*8 band_min, band_max
integer*8 vk_min, vk_max
integer*8 i, j, k, m, b
integer*8 ne, cont, nonzero, zerocont
integer*8 sum_LS, dummy
```

```
! Variables for the statistics
real*8 mean, var, stdv

! Variables for the histogram
real*8 dim_inth, minint, maxint
integer*8 cont_h, dimh
integer*8, allocatable :: freq(:)
real*8, allocatable :: freq1(:)
real*8 sumtot, distV
! Variables de Tiempo
real*8 :: start, finish

! Files
!open(101,file='silicon-spaghetti_ene.dat',status='unknown')
!open(101,file='Eu-U0.spaghettiup_ene',status='unknown')
open(101,file='Eu-spaghettiup_ene.dat',status='old')
open(102,file='HistogramLS.dat',status='unknown')
open(103,file='HistogramV.dat',status='unknown')
open(104,file='HistogramNormLS.dat',status='unknown')
open(105,file='HistogramNormV.dat',status='unknown')
open(106,file='Energias.dat',status='unknown')

! ---------------------------------------------------------------------
! -------------------Initial Variables -------------------------------

input_nband = 127     ! nband is the number of energy bands
! Silicon = 151
! Eu-U0 = 77
! Eu-U4 = 127
input_nvectork = 101  ! nvectork k-vectors per band
! Lines per band in file
! Silicon = 101 + 1
! Eu-U0 = 101 + 1
! Eu-U4 = 101 + 1
d_vectork = 0.00513   ! delta vector k
```

```
! Silicon = 0.00528
! Eu-U0 = 0.01815
! Eu-U4 = 0.00513
band_min = 5                    ! Estandar = 5
band_max = input_nband - 5      ! Estandar = input_nband - 5
vk_min = 101
vk_max = 101
nband = band_max - band_min + 1
nvectork = vk_max - vk_min + 1    ! number of k vectors being &
analized

dummy = 0

b = 0
k = 0
m = 0

allocate(levelspacing((nband-1)*nvectork))
allocate(delta_ls(nvectork))
allocate(velocity(nband*(nvectork-5)))
allocate(totalenergy(input_nband,input_nvectork))
allocate(energy(nband,nvectork))

! ---------------------------------------------------------------
! ------------------- Input energies ----------------------------

CALL cpu_time(start)

write(*,*) 'Initializing.....'

call system('cls')

write(*,*) ' ------------------- Energy input ------------------ '
write(*,*) ' '

do i = 1, input_nband
```

```
do j = 1, input_nvectork+1
if (j .eq. 1) then
read(101,*)
else
read(101,*) rtrash, rtrash, rtrash, rtrash, totalenergy(i,j-1)
end if
end do
end do

do i = band_min, band_max
k = 0
b = b + 1
do j = vk_min, vk_max
k = k + 1
energy(b,k) = totalenergy(i,j)
end do
end do

ne = b*k

!do i = 1, nband
!  write(106,*) (totalenergy(i,j), j = 1, nvectork)
!end do
do i = 1, nband
write(106,*) (energy(i,j), j = 1, nvectork)
end do
close(106)

write(*,'(5x,A,I3)') 'Number of bands = ', nband
write(*,'(5x,A,I3)') 'Number of k vectors = ', nvectork
write(*,'(5x,A,F8.5)') 'Distance between k-vectors = ', d_vectork
write(*,'(5x,A,I3,A,I3,A)') 'Interval between energy bands = ', &
band_min,' - ',band_max
write(*,'(5x,A,I3,A,I3,A)') 'Interval between k-vectors = ', &
vk_min,' - ',vk_max
write(*,*) ' '
```

```
write(*,'(5x,A,I6)') 'Number of energies = ', ne
write(*,'(5x,A,F8.5,5x,A,F8.5)') 'Ene_min = ', minval(energy),&
 'Ene_max = ', maxval(energy)

! ---------------------------------------------------------------
! -------------- Level Spacing Statistics ------------------------

write(*,*) ' '
write(*,*) ' '
write(*,*) ' ------------- Levelspacing Statistics -------------- '
write(*,*) ' '

if (vk_max .lt. vk_min .or. band_max .le. band_min) then
write(*,*) ' '
write(*,*) 'Impossible to calculate distributions &
(negative range of k vectors)'
write(*,*) ' '
goto 10
end if

cont = 0
nonzero = 0
zerocont = 0
sum_LS = 0

do j = 1, nvectork
delta_ls(j) = ((energy(nband,j))-(energy(1,j))) / nband
end do

do j = 1, nvectork
do i = 1, nband-1
cont = cont + 1
levelspacing(cont) = (energy(i+1,j)-energy(i,j))!/delta_ls(j)
end do
end do
nonzero = count(levelspacing .gt. 0.0000)
```

```
zerocont = cont - nonzero

var = 0
mean = (sum(levelspacing) / (cont))! - zerocount))
do i = 1, cont
var = var + (levelspacing(i)-mean)**2
end do
var = var / (cont)! - zerocount)
stdv = SQRT(var)

!dimh = 25
!dimh = int(sqrt(real((nband-1)*nvectork)))+1
dimh = int(2*((nband-1)*nvectork)**(0.33))+1!int(sqrt(&
real((nband-1)*nvectork)))+1
dim_inth = (maxval(levelspacing)-minval(levelspacing))/dimh
cont_h = 0

write(*,'(5x,A,I6,15x,A,I6)') 'Total LS = ', cont, 'Non-zero LS = ',&
nonzero
write(*,'(5x,A,F8.5,15x,A,F8.5)') 'LS_min = ', minval(levelspacing),&
 'LS_max = ', maxval(levelspacing)
write(*,'(5x,A,F8.5,2x,A,2x,F8.5,2x,A,2x,F8.5)') &
'LS mean / var / stdv = ', mean, '/', var, '/', stdv
write(*,'(5x,A,I3,6x,A,F8.5)') 'Number of intervals = ', dimh,&
'Size of interval = ', dim_inth
write(*,*) '   ------------------------------------------------- '
write(*,'(13x,A,12x,A,12x,A)') 'Interval','Center','Histogram'
write(*,*) '   ------------------------------------------------- '

allocate(Dist_LS(dimh))

do j = 1, dimh
Dist_LS(j) = 0
minint = (j-1)*dim_inth
maxint = j*dim_inth
do i = 1, ((nband-1)*nvectork)
```

```
if (levelspacing(i) .ge. minint .and. levelspacing(i) .le. maxint) then
Dist_LS(j) = Dist_LS(j) + 1
end if
end do
if (j .eq. 1) then
Dist_LS(j) = Dist_LS(j) - zerocont
end if
write(102,*) j, minint + (maxint - minint)/2, Dist_LS(j)
write(*,'(15x,I3,14x,F8.3,15x,I6)') j, minint + (maxint - minint)/2,&
Dist_LS(j)
end do

do i = 1, dimh
cont_h = cont_h + Dist_LS(i)
end do

write(*,'(52x,A)') '---------'
write(*,'(54x,I6)') cont_h

!write(*,*) ' '
!write(*,*) 'Data normalization'
!write(*,*) ' '

close(102)
open(102,file='HistogramLS.dat',status='unknown')

sumtot = 0

allocate(freq(dimh))
allocate(freq1(dimh))

do i = 1, dimh
read(102,*) j, distV, freq(i)
sumtot = sumtot + freq(i)
end do
```

```
!print*,'The sum total is', sumtot

do i = 1, dimh
freq1(i) = freq(i)/sumtot
!  print*, freq1(i)
if(i.ge.1)then
write(104,*) i, freq1(i)
end if
end do

!call system('Plot_LS_Histogram.plt')
call system('Plot_HistogramLS.plt')

deallocate(freq)
deallocate(freq1)

! ---------------------------------------------------------------
! ----------------- Velocity Distribution -----------------------

10 continue

write(*,*) ' '
write(*,*) ' '
write(*,*) ' --------------- Velocity distribution --------------- '
write(*,*) ' '

if (nvectork .le. 2) then
write(*,*) ' '
write(*,*) 'Impossible to calculate velocity distribution'
write(*,*) ' '
goto 20
end if

cont = 0
nonzero = 0
dummy = 0
```

```
do i = 1, nband
beta = 0.0
do j = 3, nvectork-3
cont = cont + 1
velocity(cont) = (energy(i,j+1)-energy(i,j-1))/(2*d_vectork)
!    write(*,*) velocity(cont),energy(i,j+1),energy(i,j-1),d_vectork
beta = beta + (velocity(cont))**2
if (velocity(cont) .gt. 0.0) then
nonzero = nonzero + 1
end if
end do
do k = 3, nvectork-3
dummy = dummy + 1
velocity(dummy) = velocity(dummy) / beta
end do
end do

var = 0
mean = 0
stdv = 0
mean = (sum(velocity) / (cont))! - zerocount))
do i = 1, cont
var = var + (velocity(i)-mean)**2
end do
var = var / (cont)! - zerocount)
stdv = SQRT(var)

!dimh = int(sqrt(real(nband*(nvectork-5))))+1
dimh = int(2*((nband)*(nvectork-5))**(0.33))+1
dim_inth = (maxval(velocity)-minval(velocity))/dimh
cont_h = 0
k = 0

write(*,'(5x,A,I6,15x,A,I4)') 'Total V = ', cont, 'Non-zero V = ',&
nonzero
```

```
write(*,'(5x,A,F8.5,15x,A,F8.5)') 'V_min = ', minval(velocity),&
'V_max = ', maxval(velocity)
write(*,'(5x,A,F8.5,2x,A,2x,F8.5,2x,A,2x,F8.5)') 'V mean / var / &
stdv = ', mean, '/', var, '/', stdv
write(*,'(5x,A,I3,5x,A,F8.5)') 'Number of intervals = ', dimh,&
'Size of the interval = ', dim_inth
write(*,*) '   ------------------------------------------------------ '
write(*,'(13x,A,12x,A,12x,A)') 'Interval','Center','Histogram'
write(*,*) '   ------------------------------------------------------ '

allocate(Dist_V(dimh))

do j = 1, dimh
Dist_V(j) = 0
minint = minval(velocity)+(j-1)*dim_inth
maxint = minval(velocity)+j*dim_inth
do i = 1, ((nband)*nvectork-5)
if (velocity(i) .ge. minint .and. velocity(i) .le. maxint) then
Dist_V(j) = Dist_V(j) + 1
end if
end do
write(103,'(15x,I3,14x,F8.5,15x,I6)') j, minint + (maxint - minint)/2,&
Dist_V(j)
write(*,'(15x,I3,14x,F8.5,15x,I6)') j, minint + (maxint - minint)/2,&
Dist_V(j)
end do

do i = 1, dimh
cont_h = cont_h + Dist_V(i)
end do

write(*,'(52x,A)') '---------'
write(*,'(54x,I6)') cont_h

!write(*,*) ' '
!write(*,*) 'Data normalizaion'
```

```
!write(*,*) ' '

close(103)
open(103,file='HistogramV.dat',status='unknown')

sumtot = 0

allocate(freq(dimh))
allocate(freq1(dimh))

do i = 1, dimh
read(103,*) j, rtrash, freq(i)
sumtot = sumtot + freq(i)
end do

!print*,'The sum total is', sumtot

do i = 1, dimh
minint = minval(velocity)+(j-1)*dim_inth
maxint = minval(velocity)+j*dim_inth
freq1(i) = freq(i)/sumtot
write(105,*) i, minint + (maxint - minint)/2, freq1(i)
end do

!call system('Plot_V_Histogram.plt')
call system('Plot_HistogramV.plt')

! ---------------------------------------------------------------------
! -------------------- Close and time ---------------------------
20 continue

CALL cpu_time(finish)
write(*,*) ' '
write(*,*) ' '
write(*,'(1x,A,F8.5,1x,A)') 'Elapsed time =', finish-start, 's'
```

```
!call system('plot_ls_histogram.plt')
!call system('plot_v_histogram.plt')
!call system('gfortran HistoNormalization.f90 -o Normalization.exe')
!call system('Normalization.exe')

close(101)
close(102)
close(103)
close(104)
close(105)

call system('del HistogramLS.dat')
call system('del HistogramV.dat')
call system('del HistogramNormLS.dat')
call system('del HistogramNormV.dat')
end program
```

Appendix B

Additional Figures

This appendix provides more figures that can be viewed to analyze further the data provided. The first figures are the band structures of Si and Eu with a smaller energy range in order to see the bands around the E_F more clearly. Afterwards the density of states of Si is shown.

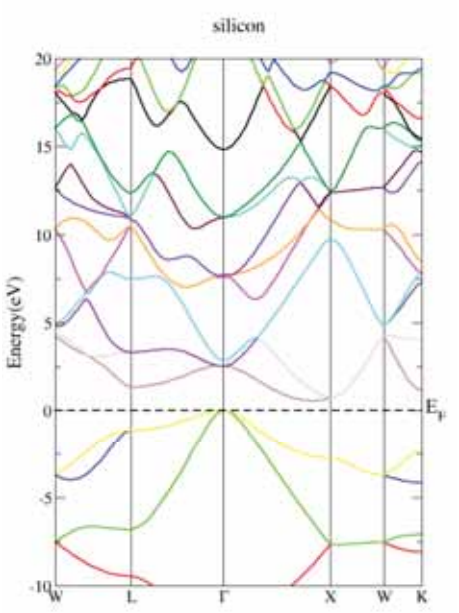

Figure B.1: Complete band structure of Si for 151 high-energy bands.

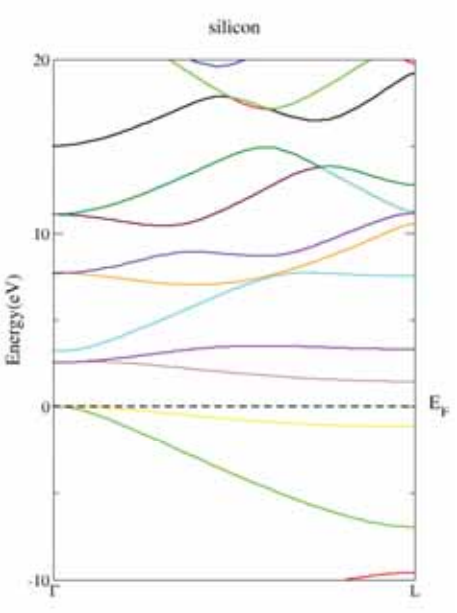

Figure B.2: Band structure of Si from Γ to L.

The band structure of Si of Figure B.2 closely resembles the one seen in literature (Mucciolo et al., 1994).

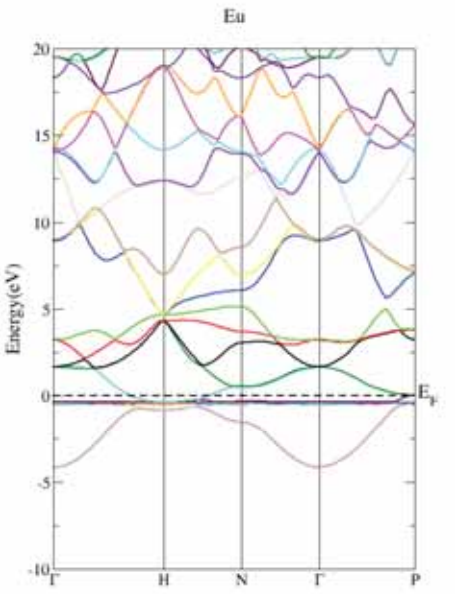

Figure B.3: Complete band structure of Eu with U = 0 for 77 high-energy bands.

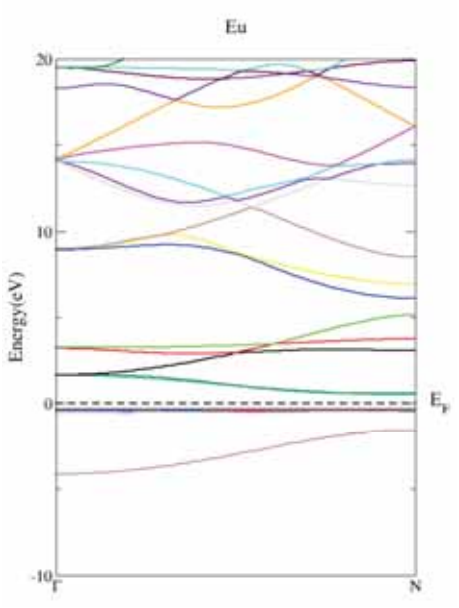

Figure B.4: Band structure of Eu with U = 0 from Γ to L for 77 high-energy bands.

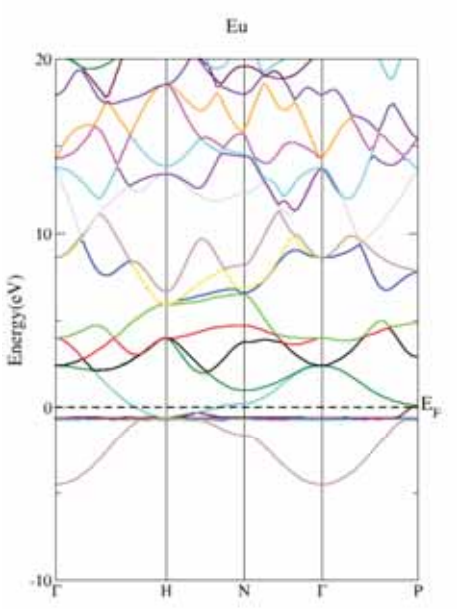

Figure B.5: Complete band structure of Eu with U = 4 for 127 high-energy bands.

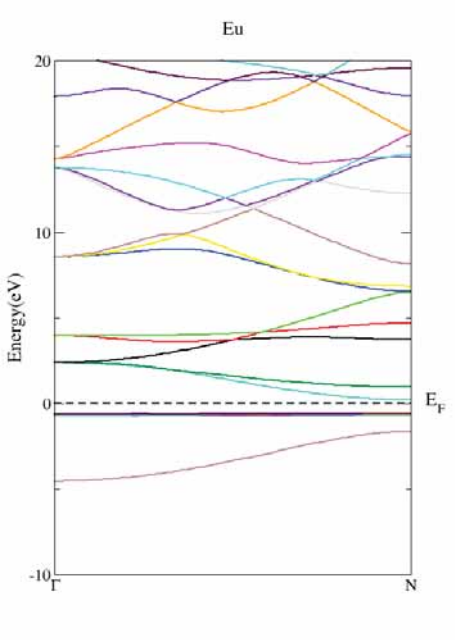

Figure B.6: Band structure of Eu with U = 4 from Γ to L for 127 high-energy bands.

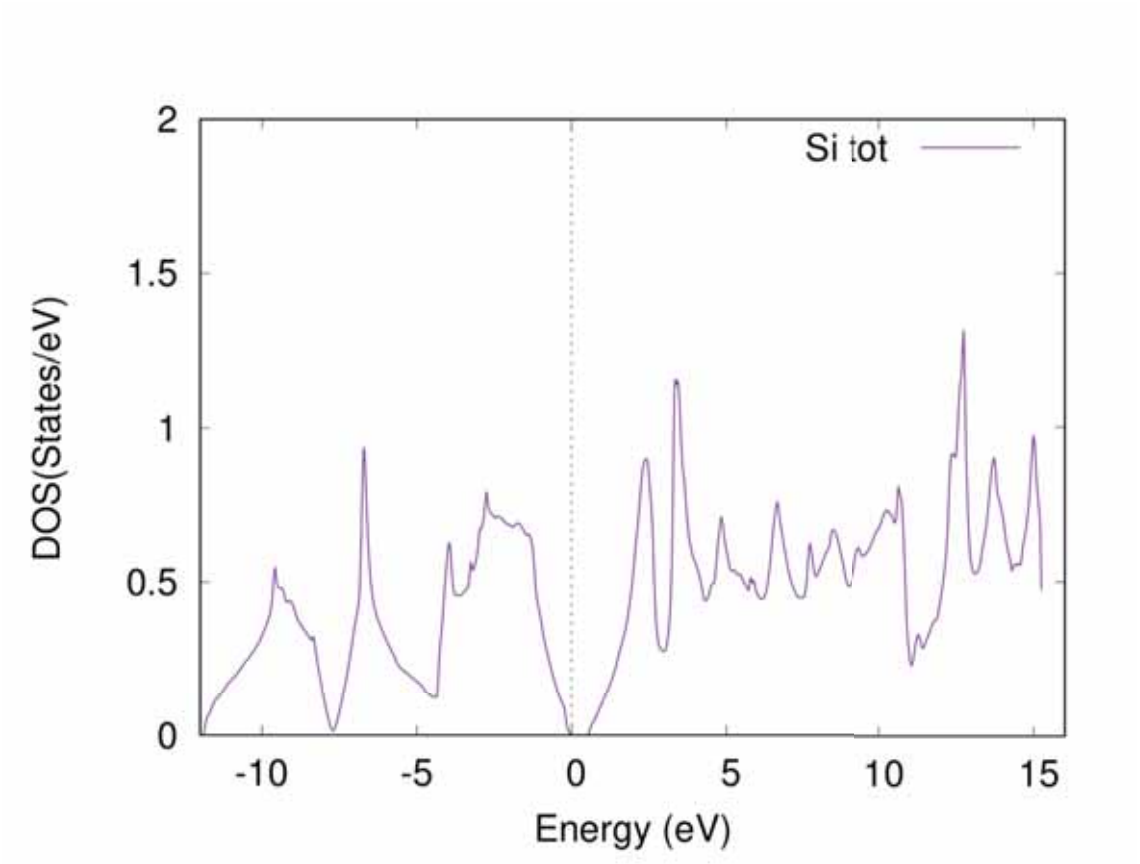

Figure B.7: Density of states of Si.

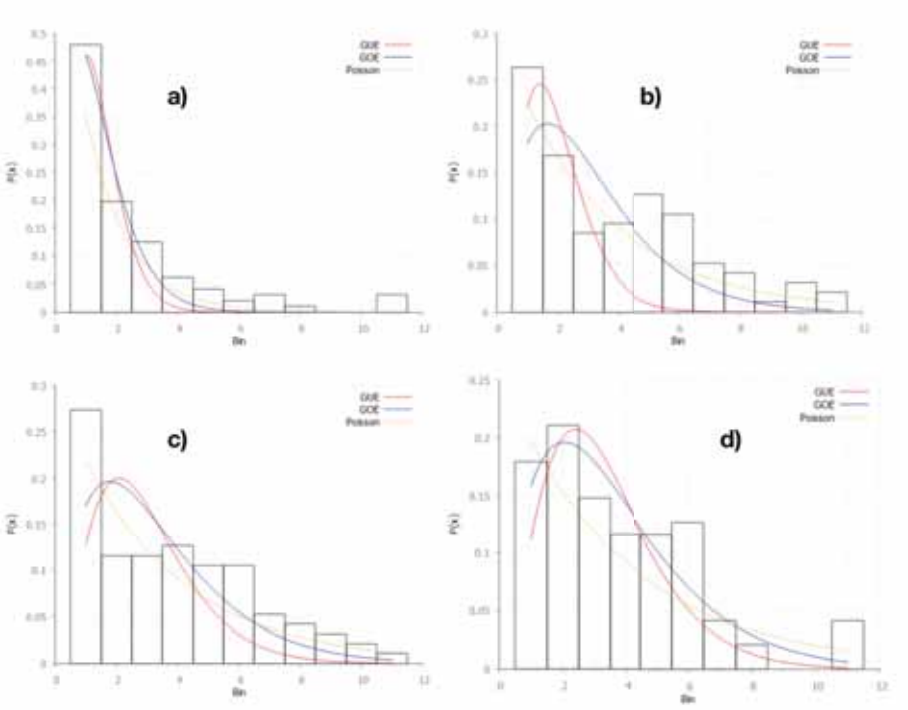

Figure B.8: Transition to chaos for Si. a) k=10, b) k=30, c) k=50, d) k=70. Si does manifest chaos when k=70

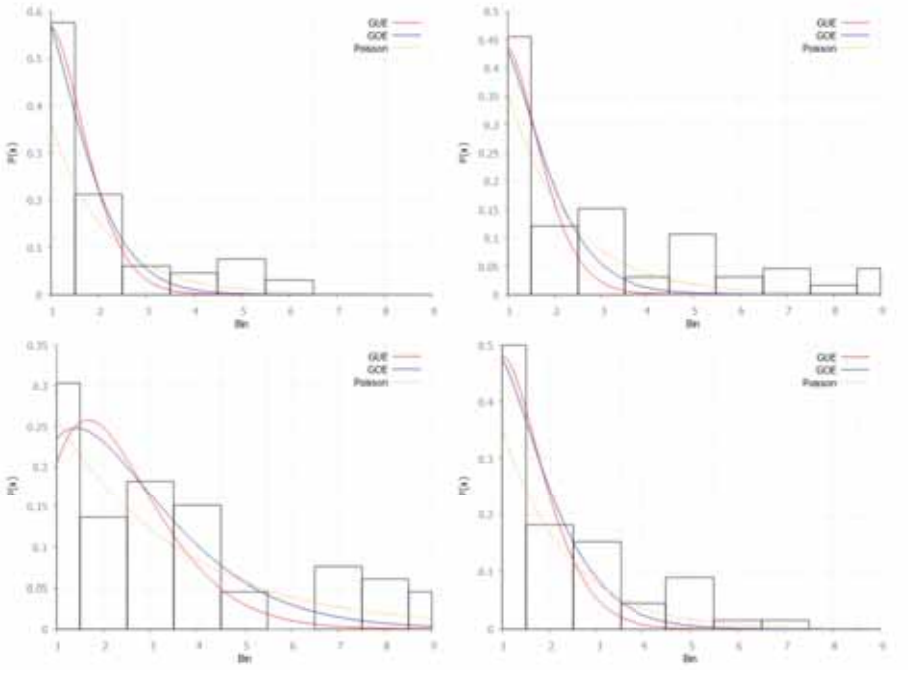

Figure B.9: Transition to chaos for Eu with $U = 0$. a) k=10, b) k=30, c) k=50, d) k=70.

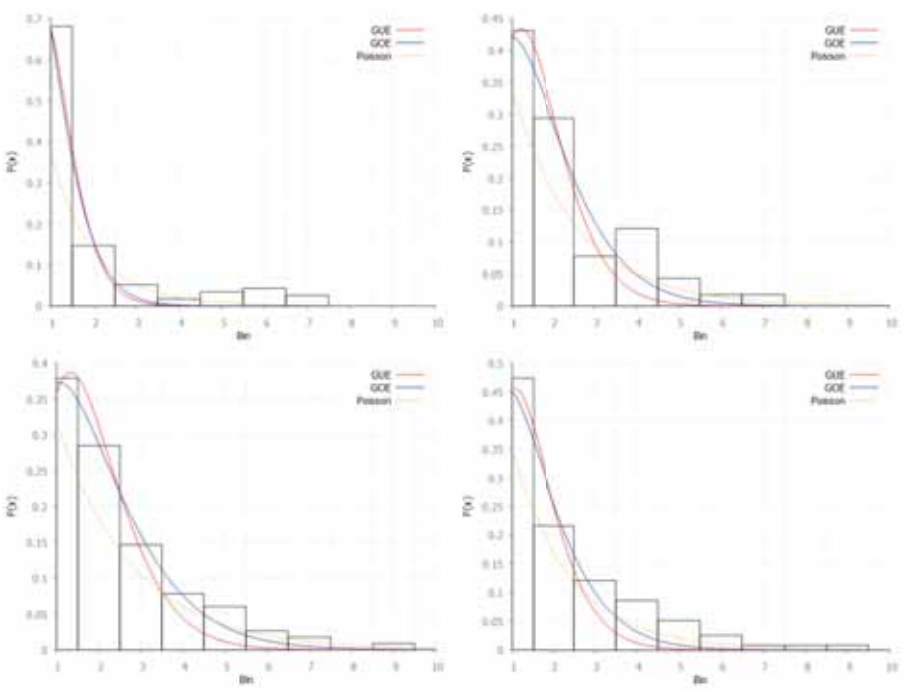

Figure B.10: Transition to chaos for Eu with $U = 4$. a) k=10, b) k=30, c) k=50, d) k=70.

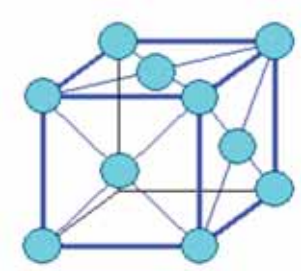

Figure B.11: Example of an FCC crystal structure similar to that of Si. (Föll)

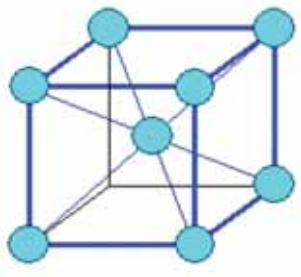

Figure B.12: Example of a BCC crystal structure similar to that of Eu. (Föll)

Bibliography

Lanthanides: Properties and reactions. URL https://chem.libretexts.org/Core/Inorganic_Chemistry/Descriptive_Chemistry/Elements_Organized_by_Block/4_f-Block_Elements/The_Lanthanides/aLanthanides%3A_Properties_and_Reactions.

Dft+u theory, 2018a. URL https://wiki.fysik.dtu.dk/gpaw/tutorials/hubbardu/hubbardu.html.

Abinit tutorial, lesson on dft+u, 2018b. URL https://www.abinit.org/sites/default/files/infos/8.0/tutorial/lesson_ldau.html.

Eu europium element information, facts, properties, trends,uses, comparison with other elements, 2018. URL https://www.schoolmykids.com/learn/interactive-periodic-table/Eu-Europium/.

G. Akemann. Random matrix theory and quantum chromodynamics. 2016. URL https://arxiv.org/pdf/1603.06011.pdf.

N. Argaman and G. Makov. Density functional theory - an introduction. URL https://arxiv.org/abs/physics/9806013v2.

M. Berry. Quantum chaology, not quantum chaos. *Physica Scripta*, 40(3):335, 1989. URL http://stacks.iop.org/1402-4896/40/i=3/a=013.

M.V. Berry and M. Tabor. Level clustering in the regular spectrum. *Proceedings of the Royal Society of London A: Mathematical, Physical and Engineering Sciences*, 356(1686):375–394, 1977. ISSN 0080-4630. doi: 10.1098/rspa.1977.0140. URL http://rspa.royalsocietypublishing.org/content/356/1686/375.

P. Blaha, K. Schwarz, G. Madsen, D. Kvasnicka, and J. Luitz. *WIEN2k: An Augmented Plane Wave Plus Local Orbitals Program for Calculating Crystal Prop-*

erties. URL https://wiki.cse.ucdavis.edu/_media/support:hpc:software:wien2k_usersguide.pdf.

G. Boeing. Visual analysis of nonlinear dynamical systems: Chaos, fractals, self-similarity and the limits of prediction. 2016. doi: 10.3390/systems4040037. URL http://www.mdpi.com/2079-8954/4/4/37.

D. Callaway. Random matrices, fractional statistics, and the quantum hall effect. 1990.

G. Casati. *Stochastic Behavior in Classical and Quantum Hamiltonian Systems*. ISBN 3-540-09120-3.

M. Côté. Introduction to dft and density functionals. URL http://pitp.physics.ubc.ca/confs/sherbrooke2012/archives/DFT-Cote.pdf.

G. Chapuis. Brillouin zone, 2017a. URL http://reference.iucr.org/dictionary/Brillouin_zone.

G. Chapuis. Wigner-seitz cell, 2017b. URL http://reference.iucr.org/dictionary/Wigner-Seitz_cell.

D. Darling. Deterministic system, 2016. URL http://www.daviddarling.info/encyclopedia/D/deterministic_system.html.

F. J. Dyson and M. L. Mehta. Statistical Theory of the Energy Levels of Complex Systems. IV. *Journal of Mathematical Physics*, 4:701–712, may 1963. doi: 10.1063/1.1704008.

H. Föll. Being iron. URL https://www.tf.uni-kiel.de/matwis/amat/iss/kap_4/backbone/r4_2_2.html.

T. Ghur, H.A. Weidenmüller, and A. Müller-Groeling. Random matrix theories in quantum physics: Common concepts. 1997.

I. S. Gomez, M. Losada, and O. Lombardi. About the concept of quantum chaos. doi: 10.3390/e19050205. URL http://www.mdpi.com/1099-4300/19/5/205.

F. Haake. *Quantum Signatures of Chaos*. Springer-Verlag. ISBN 978-3-642-05428-0. doi: 10.1007/978-3-642-05428-0.

K. Koshelev. About density functional theory interpretation. URL https://arxiv.org/abs/0812.2919.

A. I. Liechtenstein, V. I. Anisimov, and J. Zaanen. Density-functional theory and strong interactions: Orbital ordering in mott-hubbard insulators. *Phys. Rev. B*, 52:R5467–R5470, Aug 1995. doi: 10.1103/PhysRevB.52.R5467. URL https://link.aps.org/doi/10.1103/PhysRevB.52.R5467.

Steven W. McDonald and Allan N. Kaufman. Spectrum and eigenfunctions for a hamiltonian with stochastic trajectories. *Phys. Rev. Lett.*, 42:1189–1191, Apr 1979. doi: 10.1103/PhysRevLett.42.1189. URL https://link.aps.org/doi/10.1103/PhysRevLett.42.1189.

M.L. Mehta. *Random Matrices*, volume 142. Elsevier Inc., Oct 2004. ISBN 0-12-088409-7.

E. R. Mucciolo, R. B. Capaz, B. L. Altshuler, and J. D. Joannopoulos. Manifestation of quantum chaos in electronic band structures. *Phys. Rev. B*, 50:8245–8251, Sep 1994. doi: 10.1103/PhysRevB.50.8245. URL https://link.aps.org/doi/10.1103/PhysRevB.50.8245.

D.Q. Nykamp. Dynamical system definition. URL http://mathinsight.org/definition/dynamical_system.

M.A. Ocaña. Estructura electrónica de metales simples de lantánidos, 2004.

C. Oestreicher. A history of chaos theory, 2007. URL https://www.ncbi.nlm.nih.gov/pmc/articles/PMC3202497/.

T. Prosen. Chaos and complexity of quantum motion. Apr 2007.

L.E. Reichl. *The Transition to Chaos in Conservative Classical Systems: Quantum Manifestations*. Springer-Verlag, 1992. ISBN 0-387-97753-8.

D. Rickles, Penelope Hawe, and Alan Shiell. A simple guide to chaos and complexity. URL https://www.ncbi.nlm.nih.gov/pmc/articles/PMC2465602/.

Phillip Peter Rushton. Towards a non-local density functional description of exchange and correlation, 2002. URL http://cmt.dur.ac.uk/sjc/thesis_ppr/Thesis.html.

David S. Scholl and Janice A. Steckel. *Density Functional Theory A Practical Introduction*. 2009. ISBN 978-0-470-37317-0.

E. Sjöstedt, L. Nordström, and D.J. Singh. Solid state sommun. 2000.

S. H. Strogatz. *Nonlinear Dynamics and Chaos*. Perseus Books, 1994. ISBN 0-201-54344-3.

A. Szabo and N.S. Ostlund. *Modern Quantum Chemistry: Introduction to Advanced Electronic Structure*. ISBN 0-486-69186-1.

Terence Tao. *Topics in Random Matrix Theory*. American Mathematical Society, 2012. ISBN 978-0-8218-7430-1.

R. van Leeuwen. Density functional approach to the many-body problem: key concepts and exact functionals. URL `http://freescience.info/go.php?pagename=books&id=1563`.

H. A. Weidenmuller and G. E. Mitchell. Random matrices and chaos in nuclear physics. part 1. nuclear structure. *Rev. Mod. Phys.*, 81:539–589, 2009. doi: 10.1103/RevModPhys.81.539.

L. Welser-Sherrill. Astronomy of the mayans, 2007. URL `http://www.starteachastronomy.com/mayan.html`.